NSWC TR 88-252

STRENGTH AND FRACTURE CHARACTERISTICS OF HY-80, HY-100, AND HY-130 STEELS SUBJECTED TO VARIOUS STRAINS, STRAIN RATES, TEMPERATURES, AND PRESSURES

BY T. J. HOLMQUIST
(HONEYWELL INC.)

FOR NAVAL SURFACE WARFARE CENTER
RESEARCH AND TECHNOLOGY DEPARTMENT

SEPTEMBER 1987

NAVAL SURFACE WARFARE CENTER
Dahlgren, Virginia 22448-5000 • Silver Spring, Maryland 20903-5000

REPORT DOCUMENTATION PAGE

1a. REPORT SECURITY CLASSIFICATION UNCLASSIFIED	1b. RESTRICTIVE MARKINGS
2a. SECURITY CLASSIFICATION AUTHORITY	3. DISTRIBUTION/AVAILABILITY OF REPORT Approved for public release; distribution is unlimited.
2b. DECLASSIFICATION/DOWNGRADING SCHEDULE	
4. PERFORMING ORGANIZATION REPORT NUMBER(S) 32415	5. MONITORING ORGANIZATION REPORT NUMBER(S) NSWC TR 88-252
6a. NAME OF PERFORMING ORGANIZATION Honeywell Inc. Armament Systems Division 6b. OFFICE SYMBOL (If applicable)	7a. NAME OF MONITORING ORGANIZATION Naval Surface Warfare Center
6c. ADDRESS (City, State, and ZIP Code) 7225 Northland Drive Brooklyn Park, MN 55428	7b. ADDRESS (City, State, and ZIP Code) 10901 New Hampshire Avenue Silver Spring, MD 20903-5000
8a. NAME OF FUNDING/SPONSORING ORGANIZATION Naval Surface Warfare Center 8b. OFFICE SYMBOL (If applicable) Code R12	9. PROCUREMENT INSTRUMENT IDENTIFICATION NUMBER N60921-86-C-0249
8c. ADDRESS (City, State, and ZIP Code) 10901 New Hampshire Avenue Silver Spring, MD 20903-5000	10. SOURCE OF FUNDING NOS. PROGRAM ELEMENT NO. 62314N; PROJECT NO. RJ14W21; TASK NO. 5; WORK UNIT NO.
11. TITLE (Include Security Classification) Strength and Fracture Characteristics of HY-80, HY-100, and HY-130 Steels Subjected to Various Strains, Strain Rates, Temperatures, and Pressures	
12. PERSONAL AUTHOR(S) Holmquist, T. J.	
13a. TYPE OF REPORT Final	13b. TIME COVERED FROM 09/86 TO 09/87
14. DATE OF REPORT (Yr., Mo., Day) 1987, September	15. PAGE COUNT 65
16. SUPPLEMENTARY NOTATION	

17. COSATI CODES			18. SUBJECT TERMS (Continue on reverse if necessary and identify by block number)
FIELD	GROUP	SUB. GR.	Fracture Model Strength Model Computer Codes

19. ABSTRACT (Continue on reverse if necessary and identify by block number)

This report documents strength and fracture characteristics of HY-80, HY-100, and HY-130 steels subjected to various strains, strain rates, temperatures, and pressures. A series of torsion tests, Hopkinson bar tests and quasi-static tension tests were performed to obtain constants for the strength and fracture models in the EPIC-2/EPIC-3 computer codes.

20. DISTRIBUTION/AVAILABILITY OF ABSTRACT ☒ UNCLASSIFIED/UNLIMITED ☐ SAME AS RPT. ☐ DTIC USERS	21. ABSTRACT SECURITY CLASSIFICATION UNCLASSIFIED
22a. NAME OF RESPONSIBLE INDIVIDUAL Paula Walter	22b. TELEPHONE NUMBER (Include Area Code) (202) 394-2714 22c. OFFICE SYMBOL Code R12

DD FORM 1473, 84 MAR 83 APR edition may be used until exhausted. All other editions are obsolete

FOREWORD

This final report was prepared by Honeywell Inc., Armament Systems Division, 7225 Northland Drive, Brooklyn Park, Minnesota 55428, for the Naval Surface Warfare Center (NSWC), White Oak Laboratory, Silver Spring, Maryland 20903-5000, under contract N60921-86-C-0249.

This effort was conducted during the period from September 1986 to September 1987. The NSWC Program Manager was Paula Walter.

The author would like to express his appreciation to LT Josef Smith for performing the Hopkinson Bar tests at Eglin Air Force Base, and to Gordon R. Johnson and Craig Wittman of Honeywell for their contributions to his work.

The purpose of this contract was to obtain HY-80, HY-100, and HY-130 steel constants for the strength and fracture models in the EPIC-2/EPIC-3 codes.

Approved by:

Leslie A. Rockwood, Acting for

DR. KURT F. MUELLER, Head
Energetic Materials Division

CONTENTS

ILLUSTRATIONS

ILLUSTRATIONS (Cont.)

TABLES

SECTION 1

INTRODUCTION

This report documents the strength and fracture characteristics of HY-80, HY-100, and HY-130 steels, subjected to various strains, strain rates, temperatures, and pressures. The result of this characterization is the generation of constants for the strength and fracture models in the EPIC-2 and EPIC-3 codes.[1,2]

The following sections describe the test data and the analysis of the data used to obtain constants for both the strength and fracture models.

SECTION 2

TEST DATA

The test data were obtained from torsion tests at various strain rates, Hopkinson bar tension tests at various temperatures, and quasi-static tension tests with various specimen geometries (notched and unnotched). The torsion tests were performed with the Biaxial Testing Machine at Southwest Research Institute, the Hopkinson bar tests were performed at Eglin Air Force Base, and the quasi-static tension tests were performed at Honeywell. The HY-80, HY-100, and HY-130 material was provided by the Naval Surface Warfare Center (NSWC). Physical properties are given in Table 1.[3] Metallurgical data are shown in Appendix A.

Torsion data are shown in Figures 1 to 3. Comparable data for 12 other materials are presented elsewhere.[4,5] Some desirables features of this testing technique are that the state of stress in the specimen is well defined, large strains can be achieved without forming geometric instabilities, and a wide range of strain rates can be obtained with the same testing technique. It appears that adiabatic thermal softening is causing the lower stresses at the higher rates.

Figures 4 to 6 show Hopkinson bar test data at various temperatures. The elevated temperatures are obtained by surrounding the in-place test specimen by an oven such that the temperatures are applied for several minutes prior to testing. Although it is possible to test materials to greater strains than those shown in Figures 4 to 6, the Hopkinson bar data cannot be accurately evaluated after necking begins in the tensile specimens. Furthermore, at larger strains the effects of adiabatic heating can also complicate the results. The elevated temperatures show a distinct softening effect on the strength of the materials.

Photographs of the fractured Hopkinson bar specimens are shown in Figures 7 to 9. The cross-sectional area of these surfaces can be used to obtain fracture characteristics.

Quasi-static stress-strain data for both tension and torsion tests are shown in Figures 10 to 12. An equivalent tensile flow stress is obtained from the torsion data by using the von Mises flow rule, the tensile stress is $\sigma = \sqrt{3}\tau$, and the corresponding tensile strain is $\varepsilon = \gamma/\sqrt{3}$.

The stress for the tension test data is based on the current area of the neck, and the strain is defined as $\ln (A_o/A)$, where A_o and A represent the initial and current areas of the neck. The notched tension bars give a concentration of hydrostatic tension in the test specimen.[6]

This is clearly shown in the data of Figures 10 to 12. For a specified true strain, the stress (including hydrostatic tension) increases for the notched geometry. It can also be seen that the presence of the hydrostatic tension significantly decreases the strain at which the material fractures.

TABLE 1. PHYSICAL PROPERTIES OF HY-80, HY-100, AND HY-130 STEEL

		HY-80 STEEL	HY-100 STEEL	HY-130 STEEL
HARDNESS	(ROCKWELL)	C-21	C-25	C-30
ELASTIC PROPERTIES				
ELASTIC MODULUS, E	(GPa)	207	207	207
POISSON'S RATIO, υ		.30	.30	.30
SHEAR MODULUS, $E / 2 (1 + \upsilon)$	(GPa)	79	79	79
BULK MODULUS, $E / 3 (1 - 2\upsilon)$	(GPa)	172	172	172
THERMAL PROPERTIES				
DENSITY, ρ	(kg/m^3)	7746	7746	7885
CONDUCTIVITY, k	(W/mK)	34	34	27
SPECIFIC HEAT, c_p	(J/kgK)	502	502	489
DIFFUSIVITY, $k / \rho c_p$	(m^2/s)	.000009	.000009	.000007
EXPANSION COEF. (VOL.), α	(K^{-1})	.000011	.000014	.000013
MELTING TEMPERATURE, T_{MELT}	(K)	1793	1793	1793

N07-020.JF

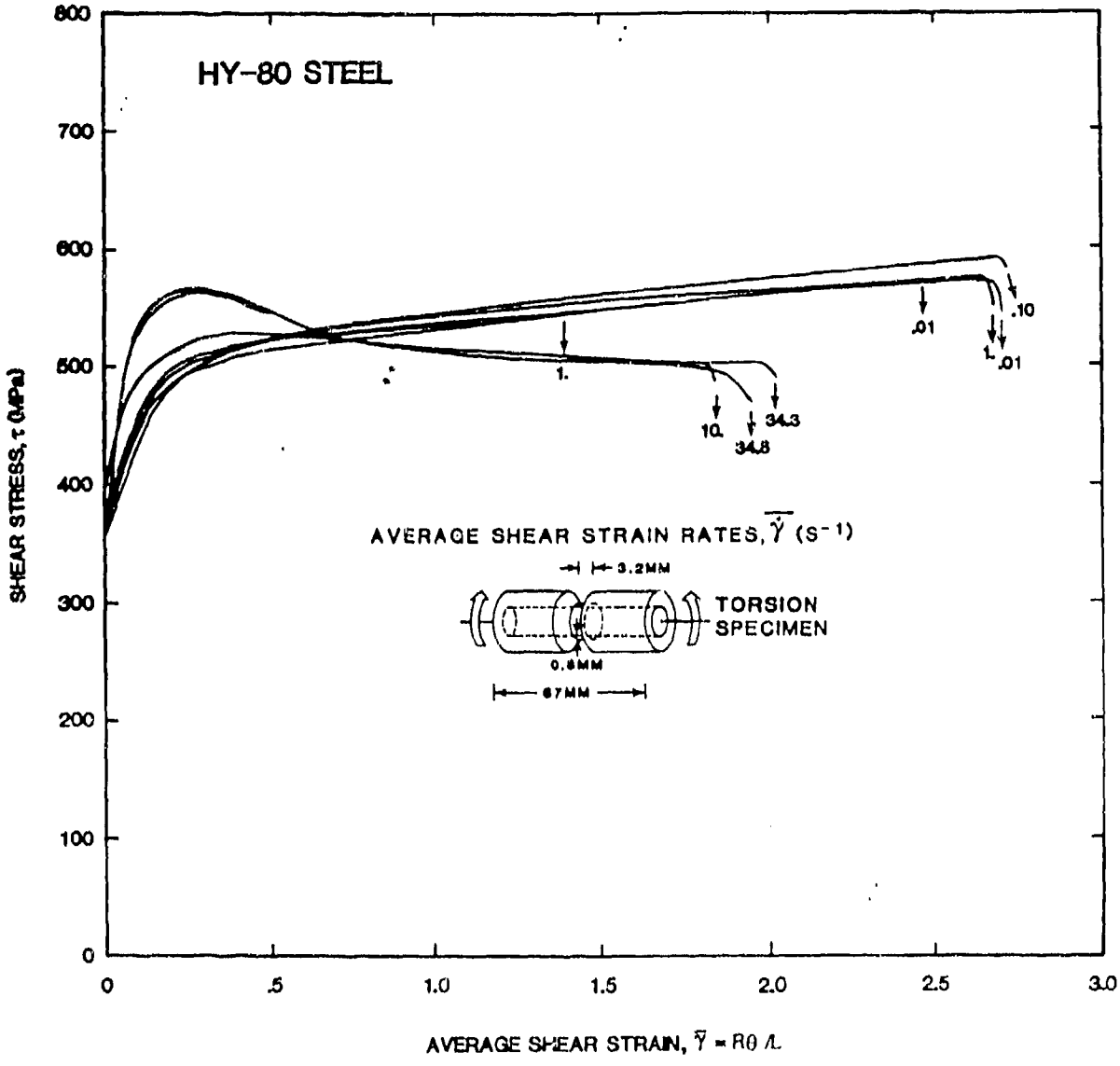

FIGURE 1. STRESS-STRAIN DATA FOR TORSION TESTS AT VARIOUS STRAIN RATES FOR HY-80 STEEL

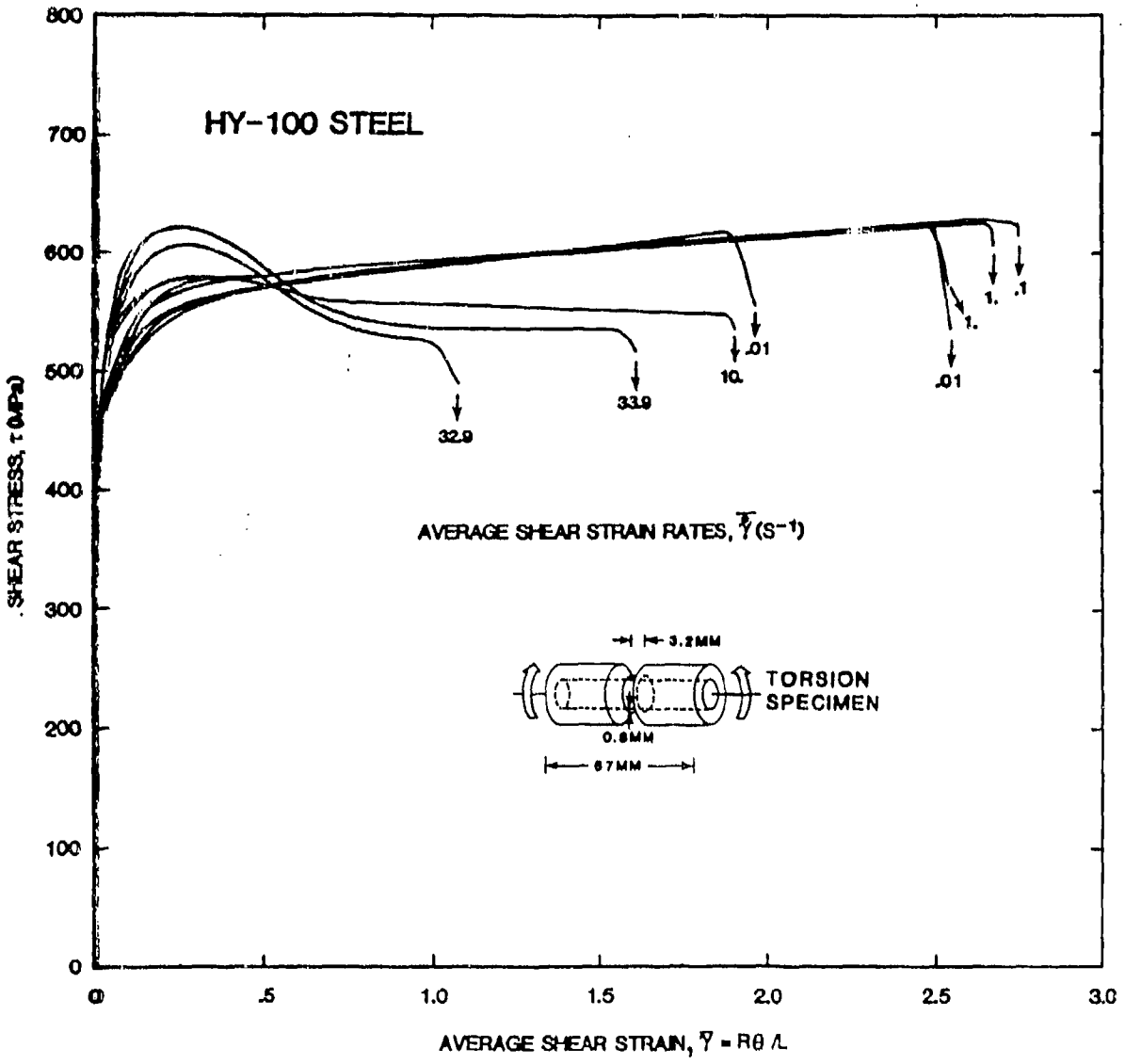

FIGURE 2. STRESS-STRAIN DATA FOR TORSION TESTS AT VARIOUS STRAIN RATES FOR HY-100 STEEL

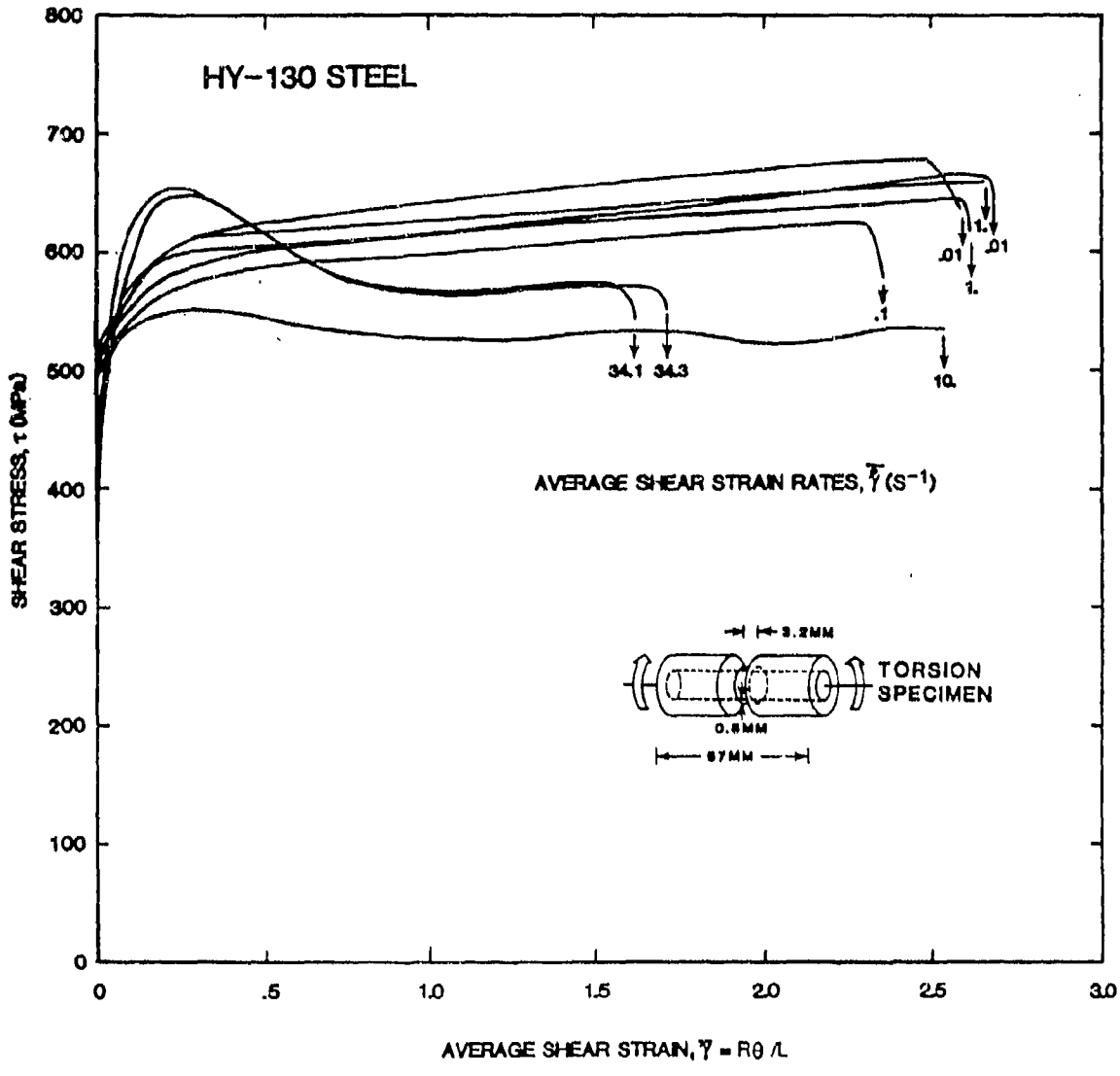

FIGURE 3. STRESS-STRAIN DATA FOR TORSION TESTS AT VARIOUS STRAIN RATES FOR HY-130 STEEL

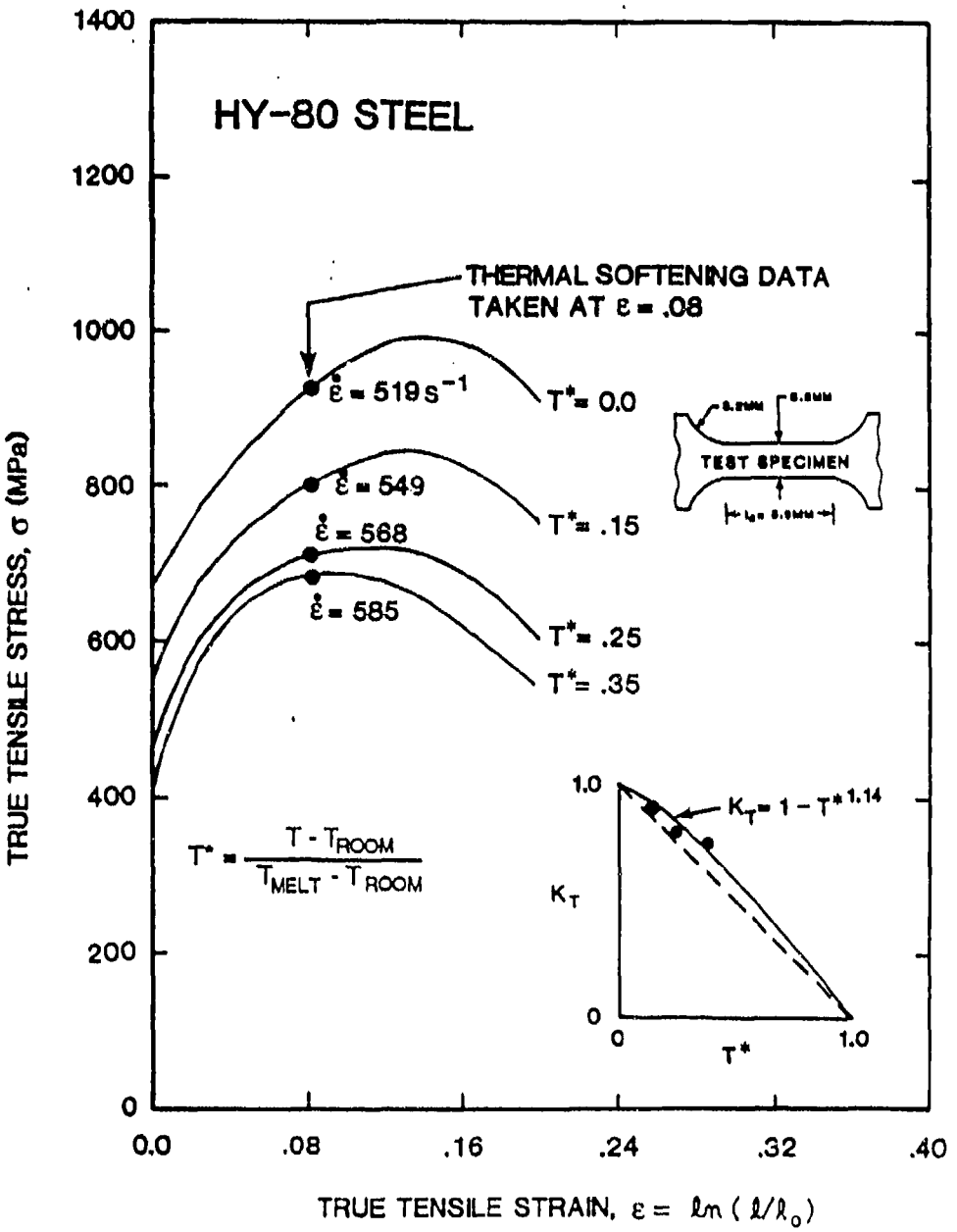

FIGURE 4. STRESS-STRAIN DATA FOR HOPKINSON BAR TESTS AT VARIOUS TEMPERATURES FOR HY-80 STEEL

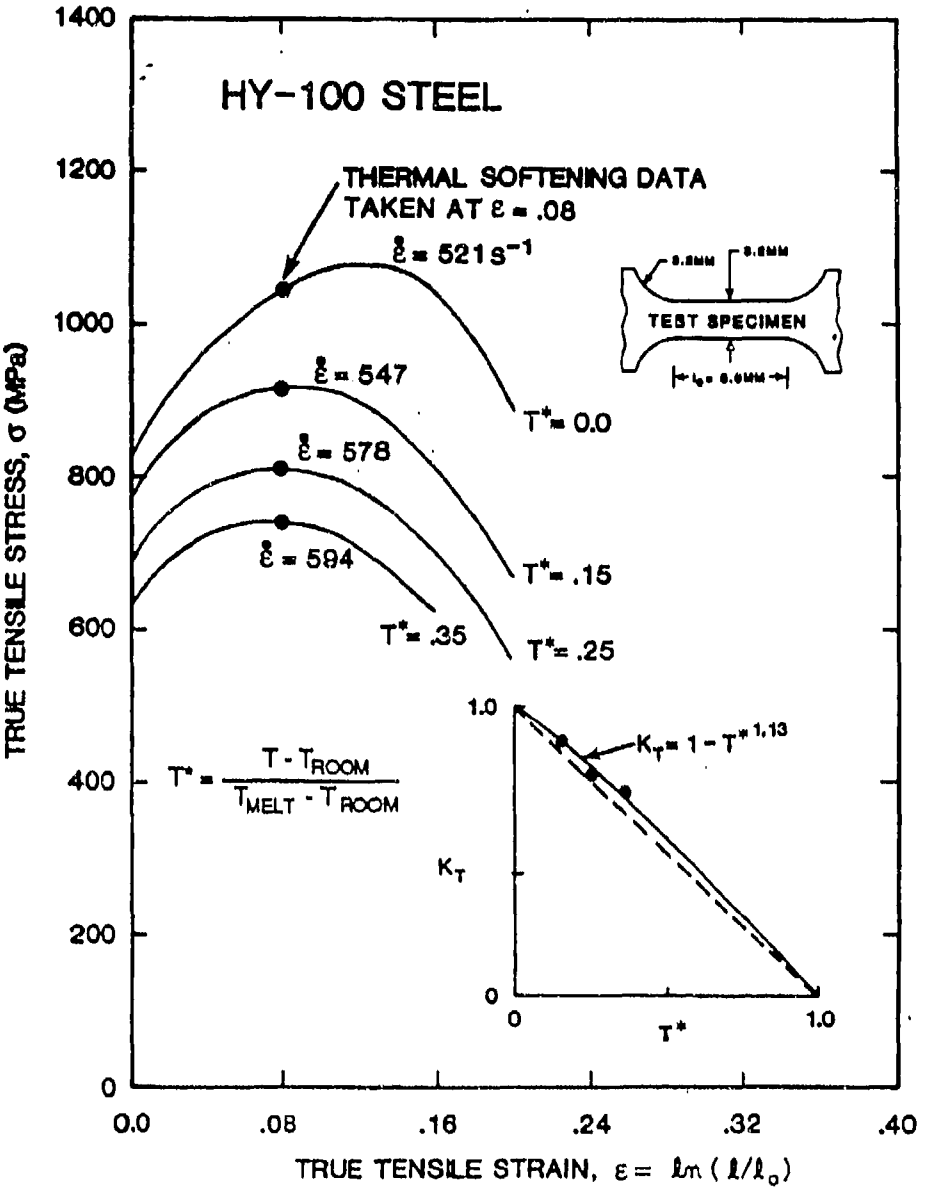

FIGURE 5. STRESS-STRAIN DATA FOR HOPKINSON BAR TESTS AT VARIOUS TEMPERATURES FOR HY-100 STEEL

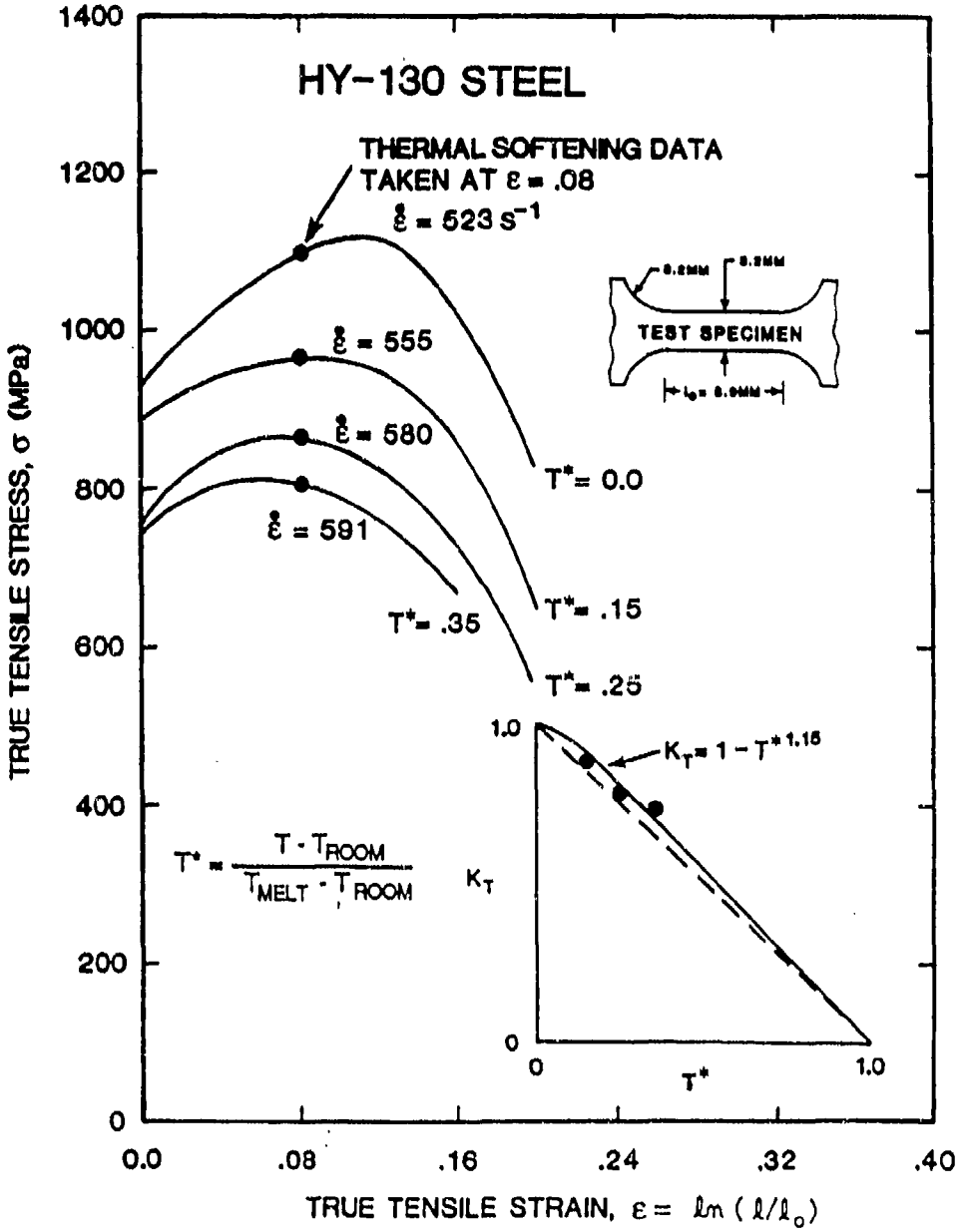

FIGURE 6. STRESS-STRAIN DATA FOR HOPKINSON BAR TESTS AT VARIOUS TEMPERATURES FOR HY-130 STEEL

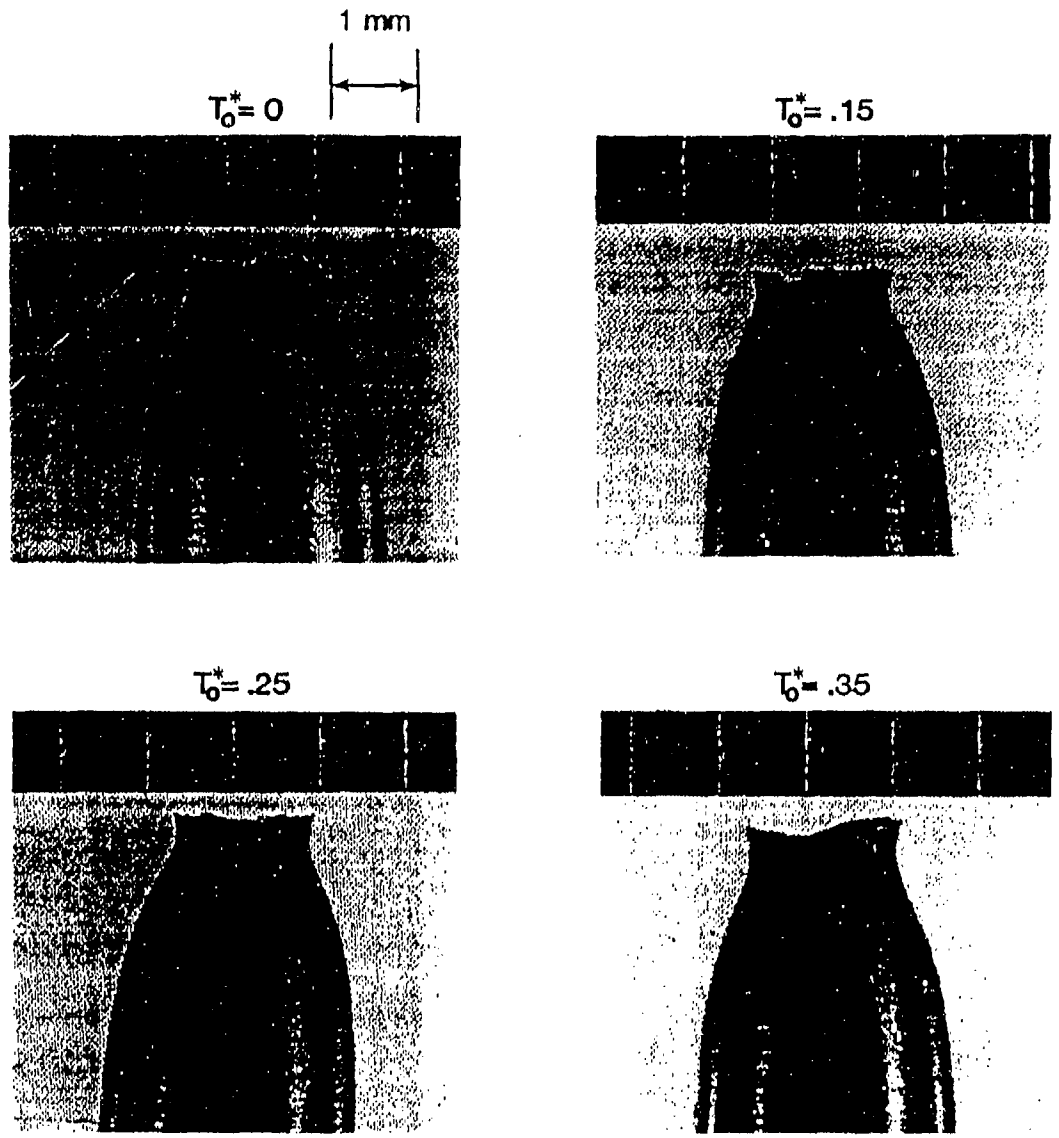

FIGURE 7. PHOTOGRAPHS OF THE FRACTURE PROFILES ON THE HY-80 STEEL HOPKINSON BAR SPECIMENS

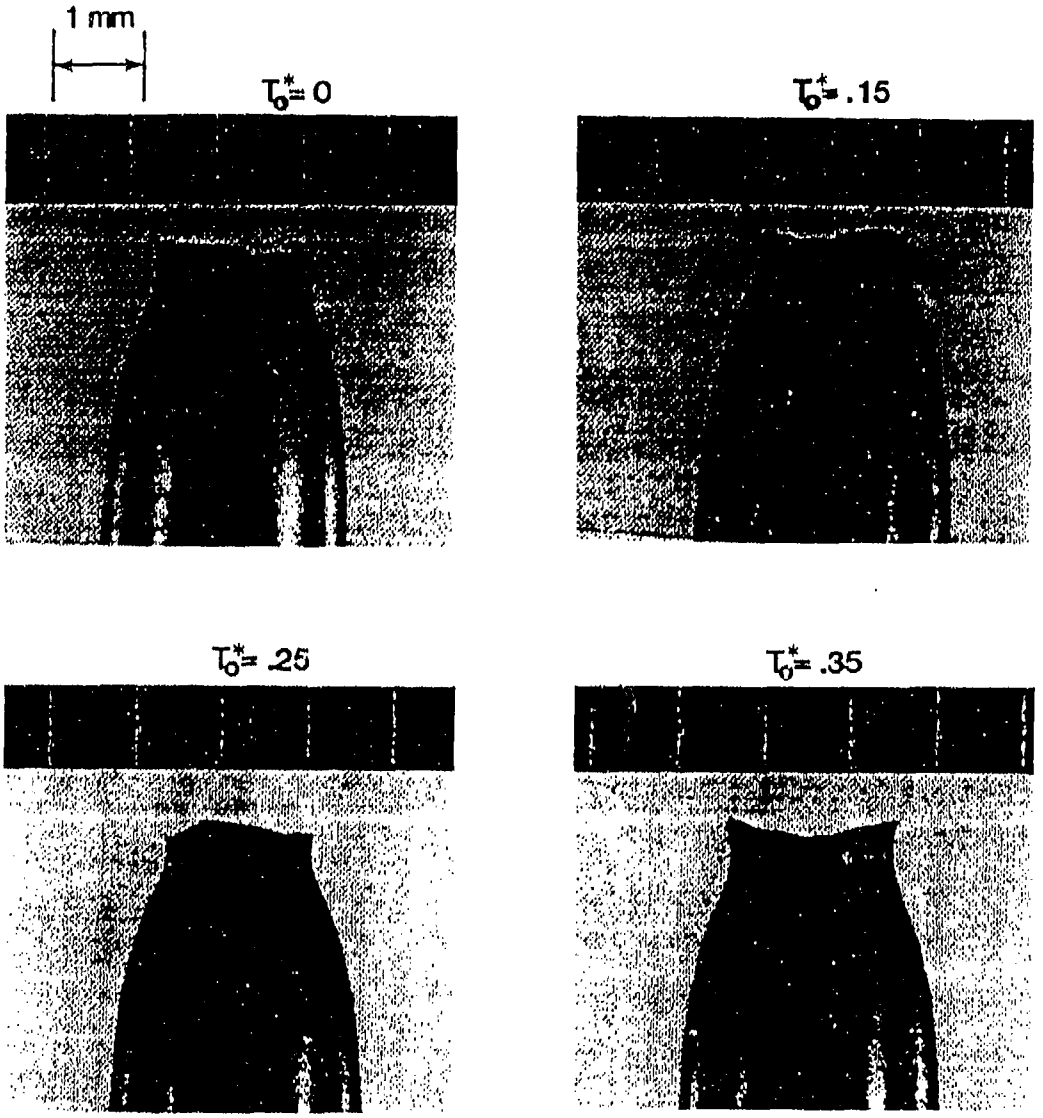

FIGURE 8. PHOTOGRAPHS OF THE FRACTURE PROFILES ON THE HY-100 STEEL HOPKINSON BAR SPECIMENS

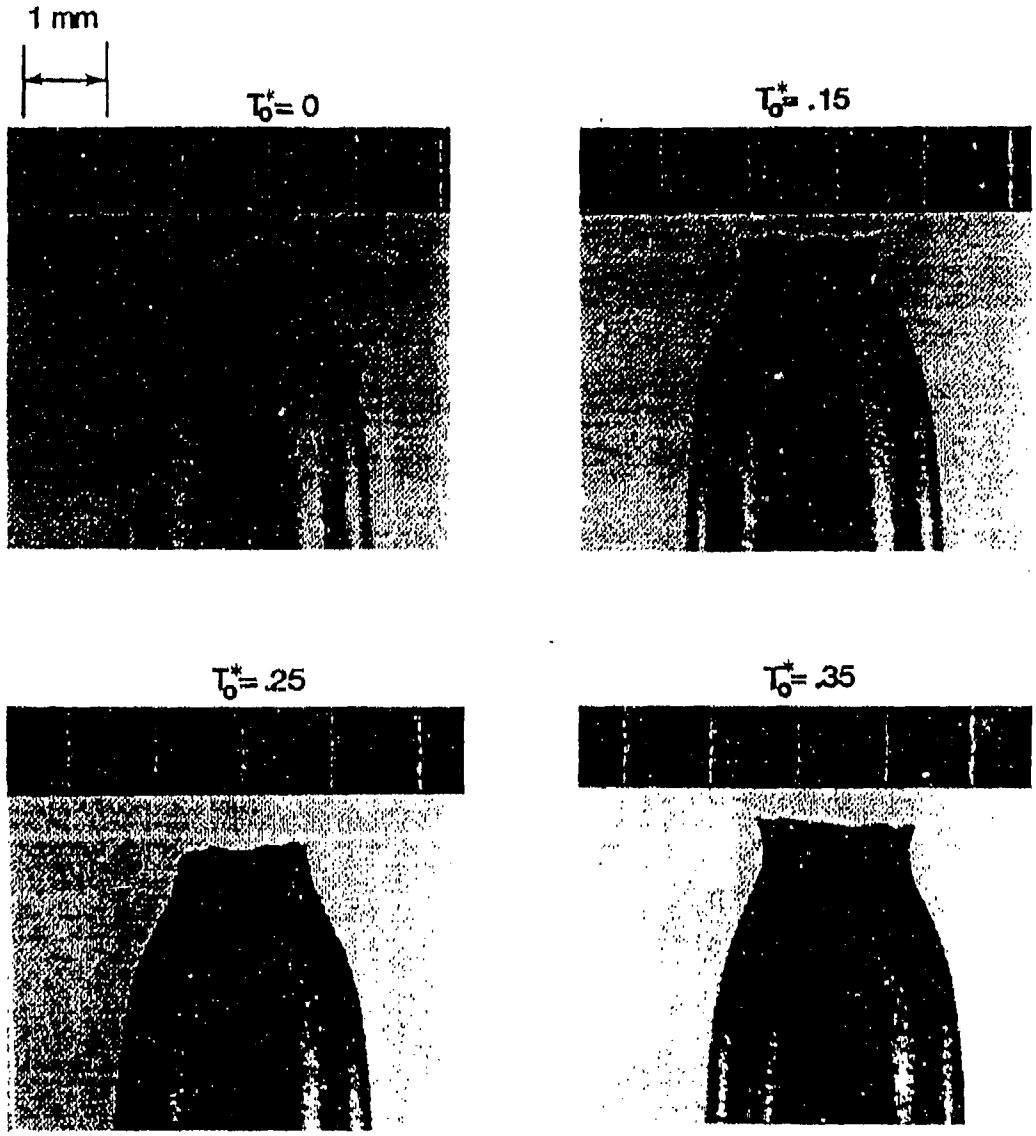

FIGURE 9. PHOTOGRAPHS OF THE FRACTURE PROFILES ON THE HY-130 STEEL HOPKINSON BAR SPECIMENS

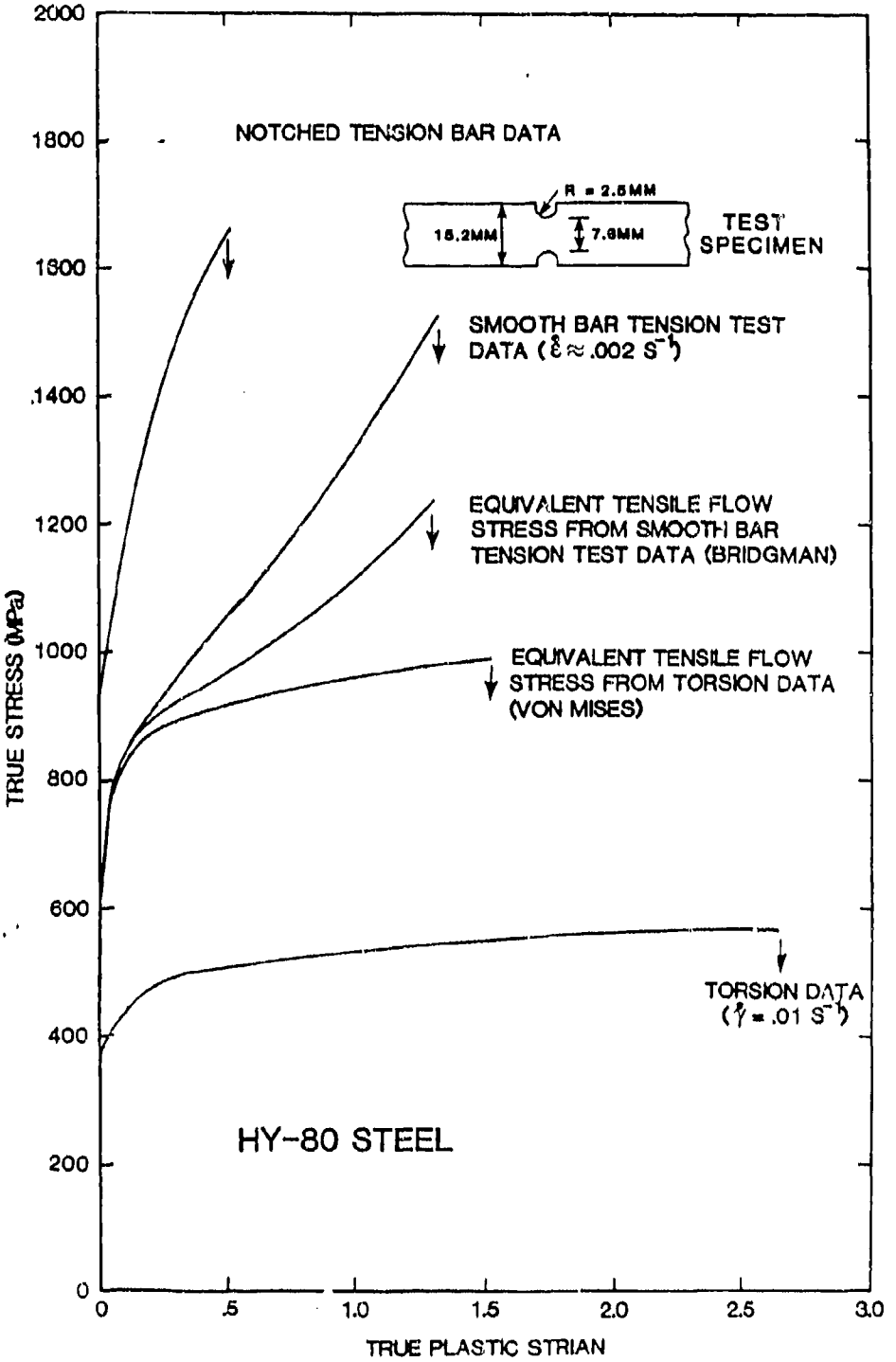

FIGURE 10. STRESS STRAIN DATA FOR QUASI-STATIC TENSION AND TORSION DATA FOR HY-80 STEEL

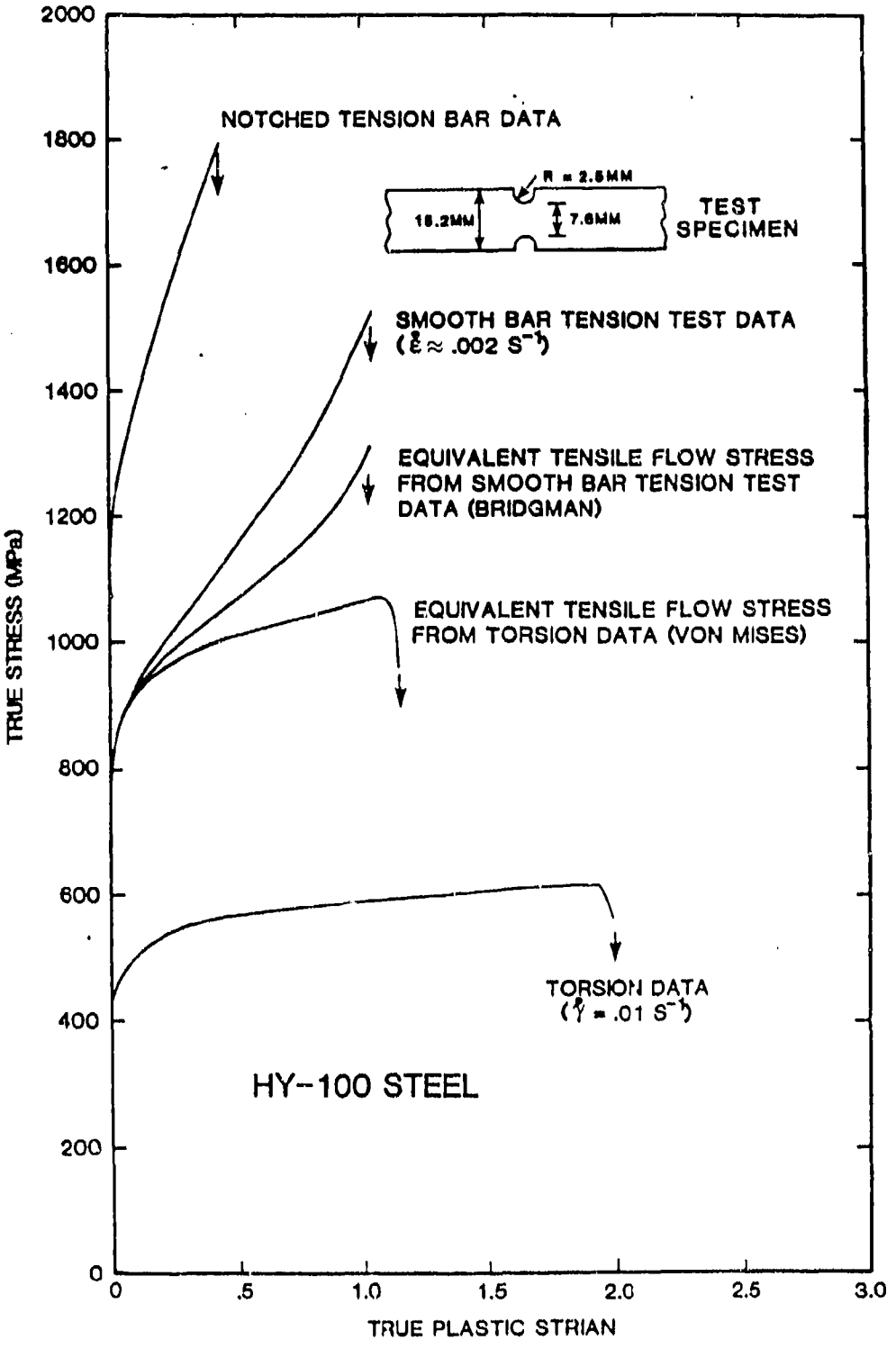

FIGURE 11. STRESS-STRAIN DATA FOR QUASI-STATIC TENSION AND TORSION DATA FOR HY-100 STEEL

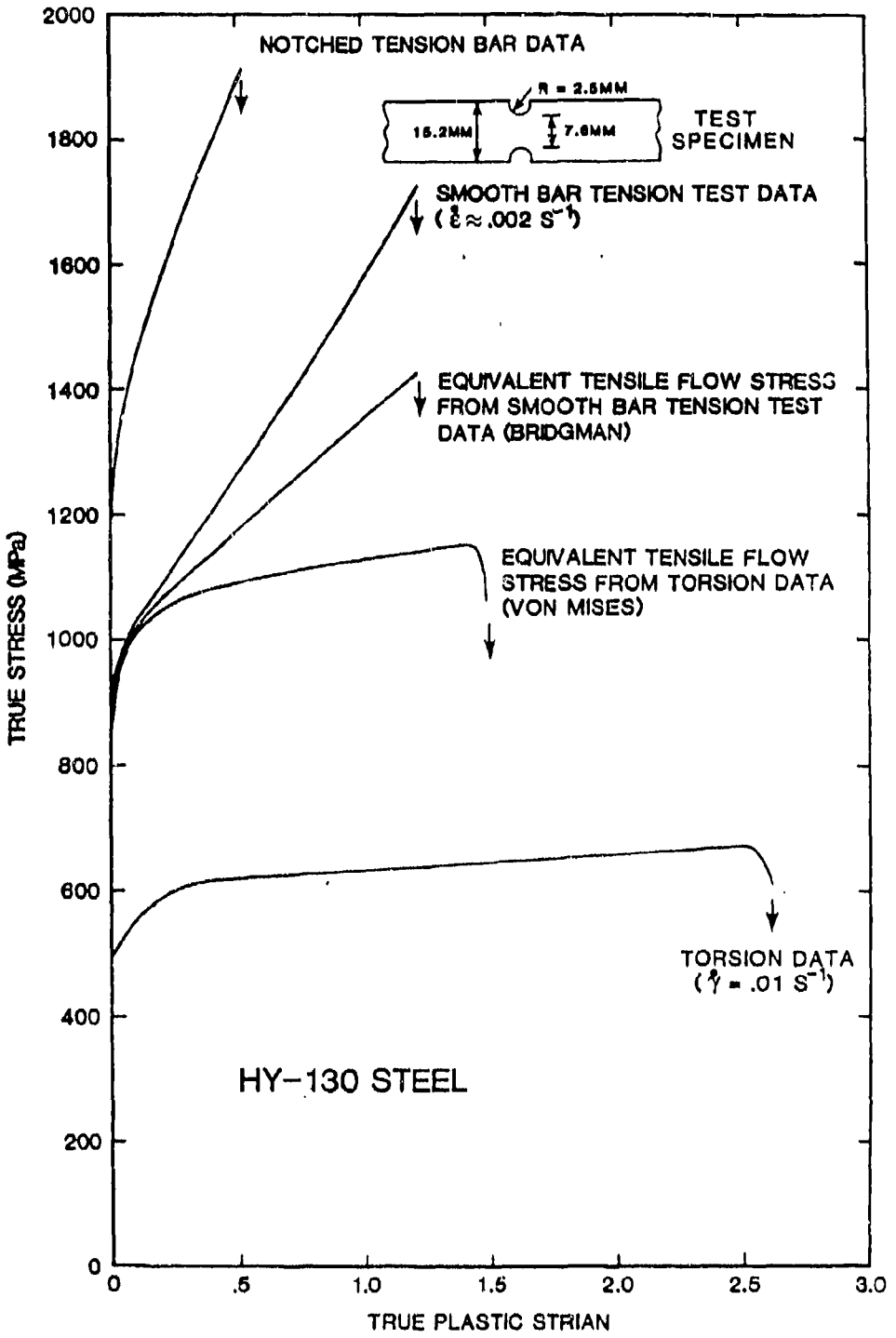

FIGURE 12. STRESS-STRAIN DATA FOR QUASI-STATIC TENSION AND TORSION DATA FOR HY-130 STEEL

SECTION 3

STRENGTH MODEL

The origin of the strength model, and the techniques used to extract constants for the model, are described in References 7 and 8. The analysis which follows is essentially identical to that described in these references.

The model for the von Mises flow stress, σ, is expressed as

$$\sigma = [A + B\varepsilon^n][1 + C\ln\dot{\varepsilon}^*][1 - T^{*m}] \quad (1)$$

where ε is the equivalent plastic strain, $\dot{\varepsilon}^* = \dot{\varepsilon}/\dot{\varepsilon}_0$ is the dimensionless plastic strain rate for $\dot{\varepsilon}_0 = 1.0s^{-1}$ and T^* is the homologous temperature. The five material constants are A, B, n, C, m. The expression in the first set of brackets gives the stress as a function of strain for $\dot{\varepsilon}^* = 1.0$ and $T^* = 0$. The expressions in the second and third sets of brackets represent the effects of strain rate and temperature, respectively. The basic form of the model is readily adaptable to most computer codes since it uses variables (ε, $\dot{\varepsilon}^*$, T^*) which are available in the codes.

The first step in the process is to determine the constants in the first set of brackets. A is the yield stress and B and n represent the effects of strain hardening. Since the torsion data in Figures 1 to 3 include the strain rate of interest ($\dot{\varepsilon}^* = 1.0$), it is a straightforward procedure to obtain the appropriate constants for this strain rate.

The same three constants can also be derived from the quasi-tension data of Figures 10 to 12. These results are for $\dot{\varepsilon}^* = 0.002$ and must therefore be adjusted for $\dot{\varepsilon}^* = 1.0$. This can readily be accomplished after the strain rate constant, C, is determined.

Figure 13 shows the effect of strain rate for tension and torsion. In both cases the stress increases as the strain rate increases. The results are shown for relatively small strain values ($\varepsilon = 0.08$, $\gamma = 0.20$) to ensure that the strain rate effect is not significantly altered by adiabatic thermal softening. Strain rate constants for both tension and torsion can be determined from the 'least squares' linear approximations of the data.

The effect of thermal softening is shown in Figures 4 to 6. The thermal softening fraction, $K_t = 1 - T^{*m}$, is simply the ratio of the stress at elevated temperature to that at room temperature. The thermal softening constant, m, is shown to give an analytic expression which closely matches the experimental data.

At this point there are two sets of constants (tension and torsion) for strain and strain rate effects (A, B, n, C) and one constant, m,for the thermal softening. Averaging the tension and torsion constants for strain rate effects gives a final set of constants (A, B, n, C) to be used in the strength model. The resulting stress-strain relationships are shown in Figures 14 to 16.

It can be seen that the strength results for the three materials are well behaved. As expected, the HY-80 steel has the lowest strength and the HY-130 has the highest strength. The yield stresses, A, increase when going from the HY-80 to the HY-130; the strain rate effects, C, decrease when going from the HY-80 to the HY-130; and the thermal softening effects, m, are essentially identical for all three materials.

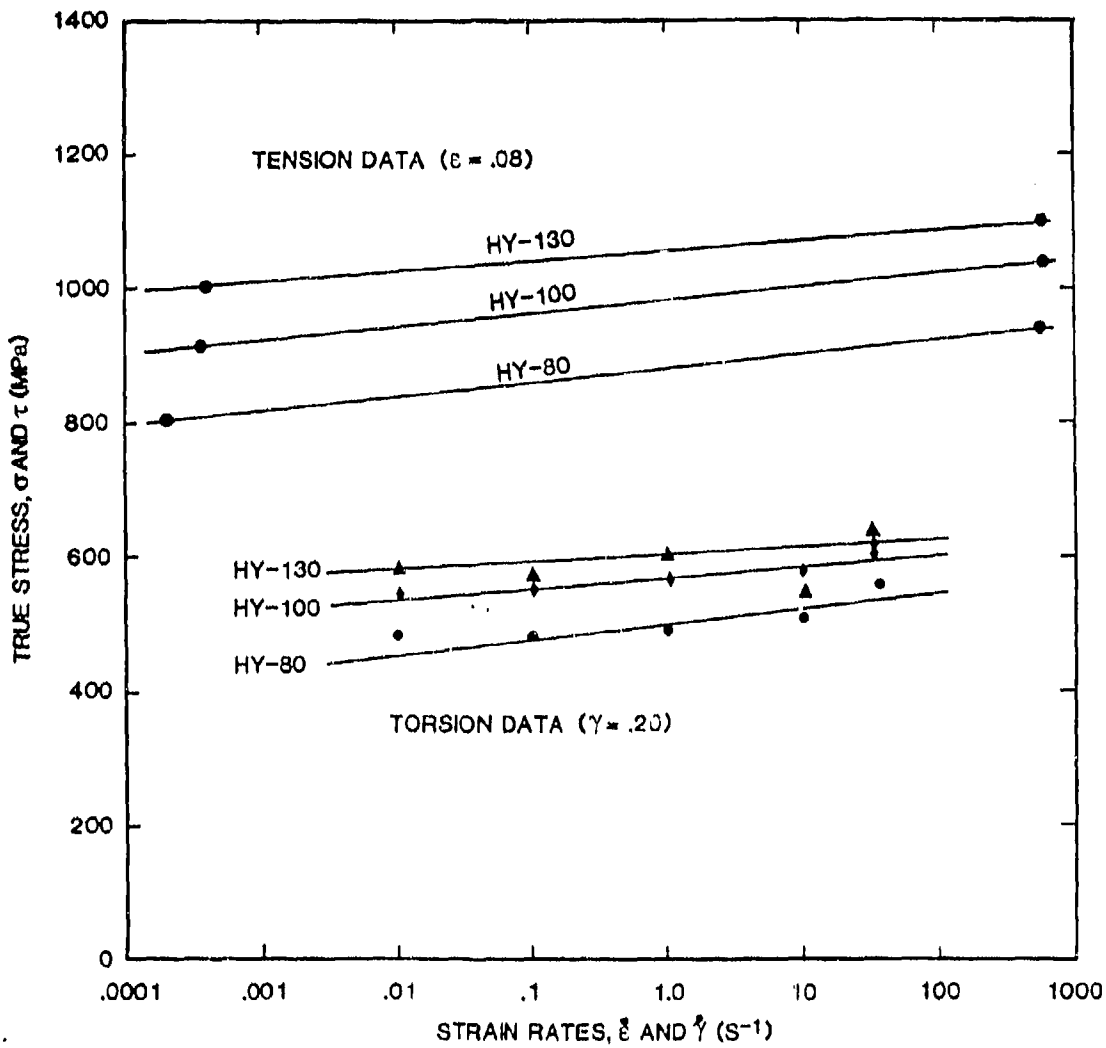

FIGURE 13. STRESS VERSUS STRAIN RATE FOR TENSION AND TORSION TESTS

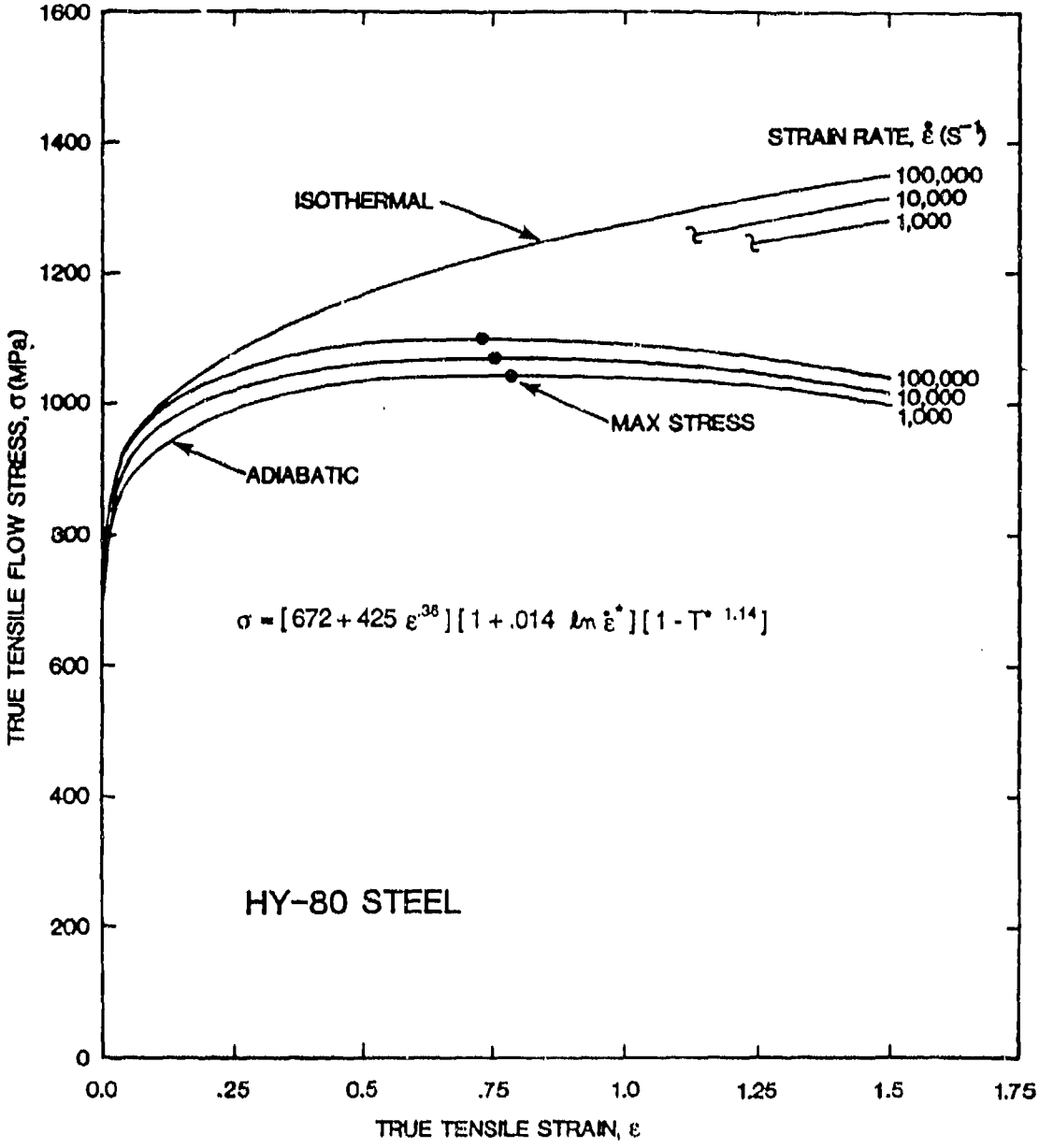

FIGURE 14. ANALYTIC STRESS STRAIN RELATIONSHIPS FOR ISOTHERMAL AND ADIABATIC CONDITIONS FOR HY-80 STEEL

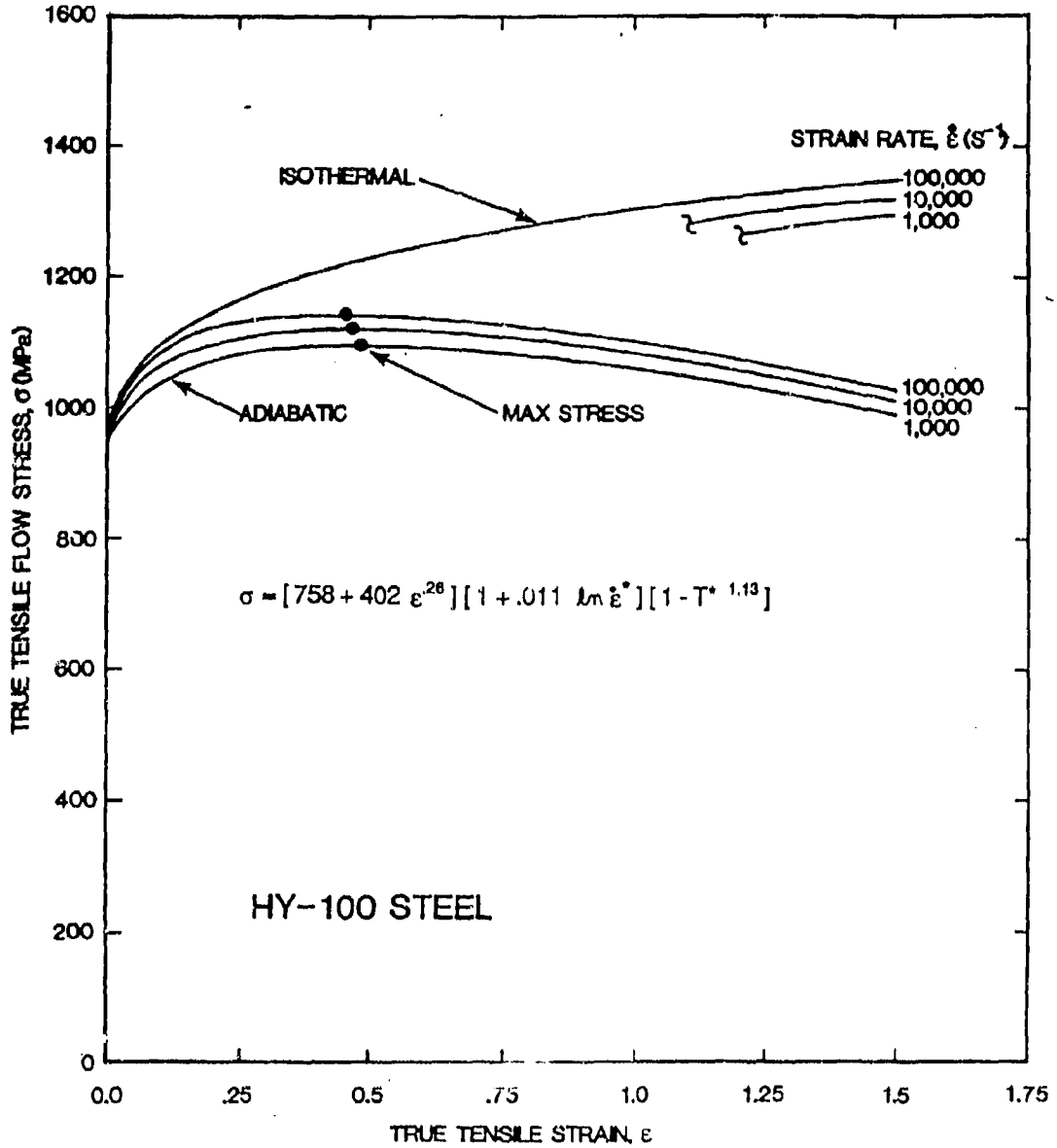

FIGURE 15. ANALYTIC STRESS-STRAIN RELATIONSHIPS FOR ISOTHERMAL AND ADIABATIC CONDITIONS FOR HY-100 STEEL

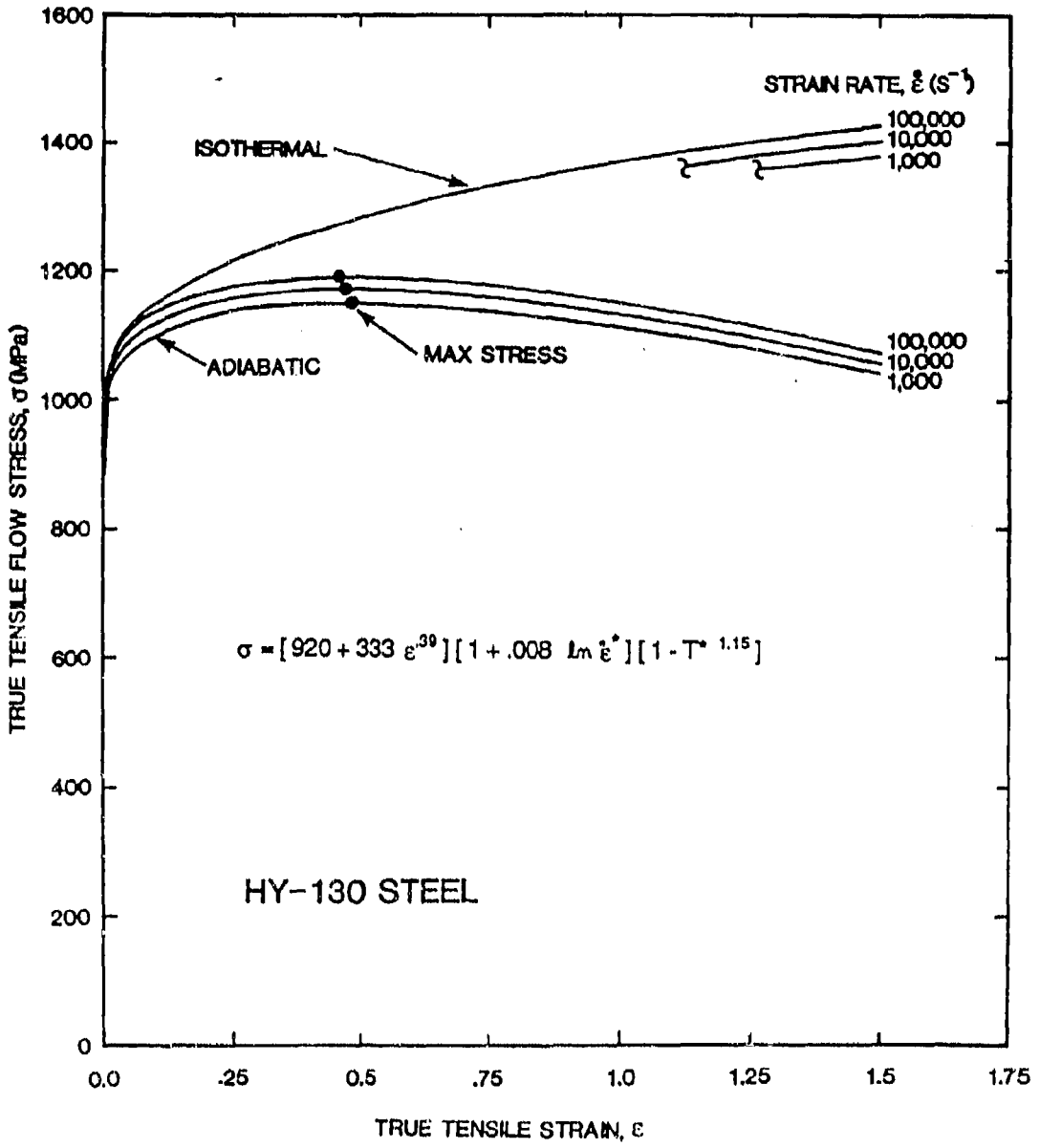

FIGURE 16. ANALYTIC STRESS-STRAIN RELATIONSHIPS FOR ISOTHERMAL AND ADIABATIC CONDITIONS FOR HY-130 STEEL

SECTION 4

FRACTURE MODEL

The origin of the fracture model and the techniques used to obtain the appropriate constants are presented in References 7 and 9. As was the case with the strength constants, the fracture constants are obtained in a manner similar to that presented in these references.

To begin, the damage to an element is defined as

$$D = \sum \frac{\Delta\varepsilon}{\varepsilon_f} \tag{2}$$

where $\Delta\varepsilon$ is the increment of equivalent plastic strain which occurs during an integration cycle, and ε_f is the equivalent strain to fracture, under the current conditions of strain rate, temperature, pressure and equivalent stress. Fracture is then allowed to occur when $D = 1.0$.

The general expression for the strain at fracture is given by

$$\varepsilon_f = [D_1 + D_2 \exp D_3\sigma^*][1 + D_4 \ln\dot{\varepsilon}^*][1 + D_5 T^*] \tag{3}$$

for constant values of the variables (σ^*, $\dot{\varepsilon}^*$, T^*) and $\sigma^* \leq 1.5$. The dimensionless pressure-stress ratio is defined as $\sigma^* = \sigma_m/\bar{\sigma}$ where σ_m is the average of the three normal stresses and $\bar{\sigma}$ is the von Mises equivalent stress. The dimensionless strain rate, $\dot{\varepsilon}^*$ and homologous temperature, T^*, are identical to those used in the strength model of Equation (1).

The five constants are $D_1 \ldots D_5$. The expression in the first set of brackets follows the form presented by Hancock and Mackenzie.[10] It essentially says that the strain to fracture decreases as the hydrostatic tension, σ_m increases. The expression in the second set of brackets represents the effect of strain rate, and that in the third set of brackets represents the effect of temperature. For high values of hydrostatic tension ($\sigma^* > 1.5$), ε_f is linearly interpolated between ε_f at $\sigma^* = 1.5$ and ε_f^{min} at $\sigma^* = \sigma_{spall}/\bar{\sigma}$, where σ_{spall} and ε_f^{min} are input values of spall stress and strain.[7,9]

The first step required to obtain the fracture constants is to determine the effect of the dimensionless pressure-stress ratio, σ^*. This can be done by considering the quasi-static tension and torsion data of Figures 10 to 12 and 17. For the torsion data $\sigma^* = 0$ and for the unnotched tension data $\sigma^* = 1/3$. For the notched tension bar, EPIC-2 simulations were performed to compute σ^* at the center of the specimen. These results are shown in Figure 18. For these computations, an average pressure for each set of adjacent triangular elements was used to eliminate any excessive stiffness due to the triangular element formulation.[11]

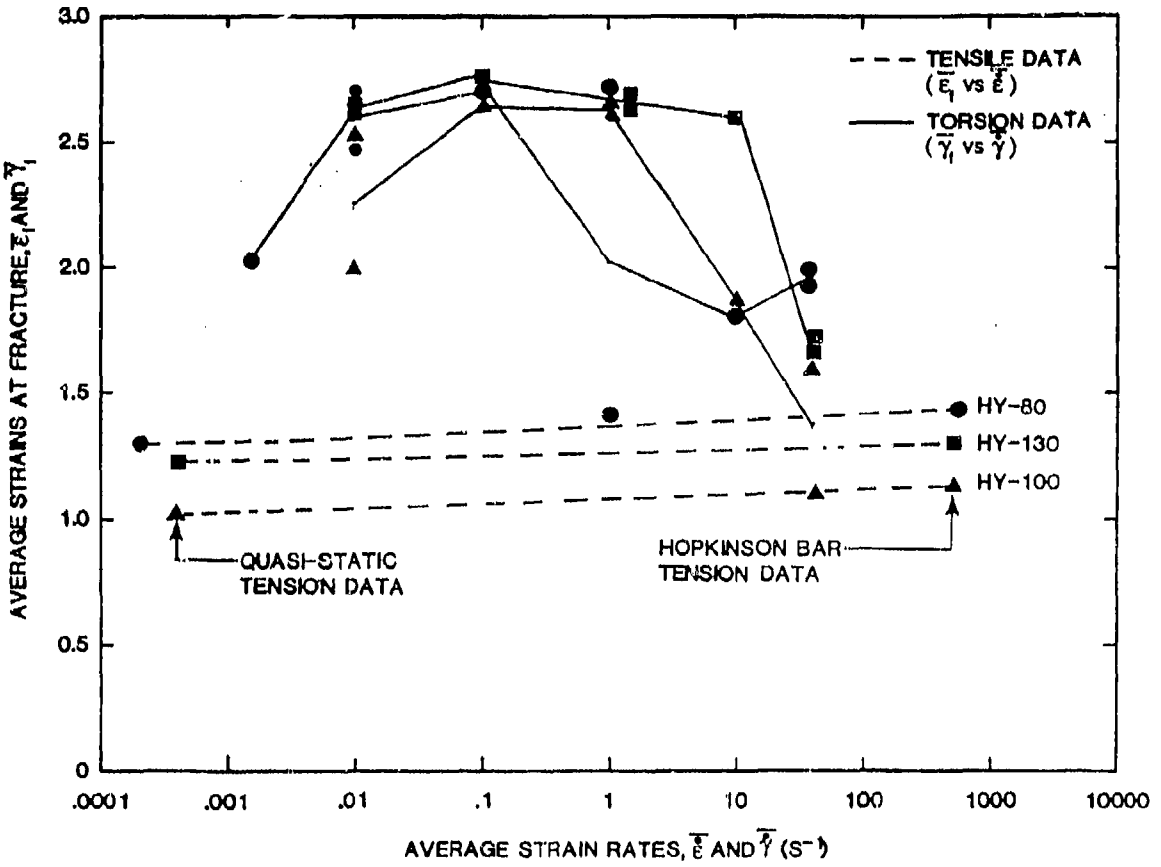

FIGURE 17. AVERAGE FRACTURE STRAIN VERSUS STRAIN RATE FOR TENSION AND TORSION TESTS FOR HY-80, HY-100, AND HY-130 STEEL

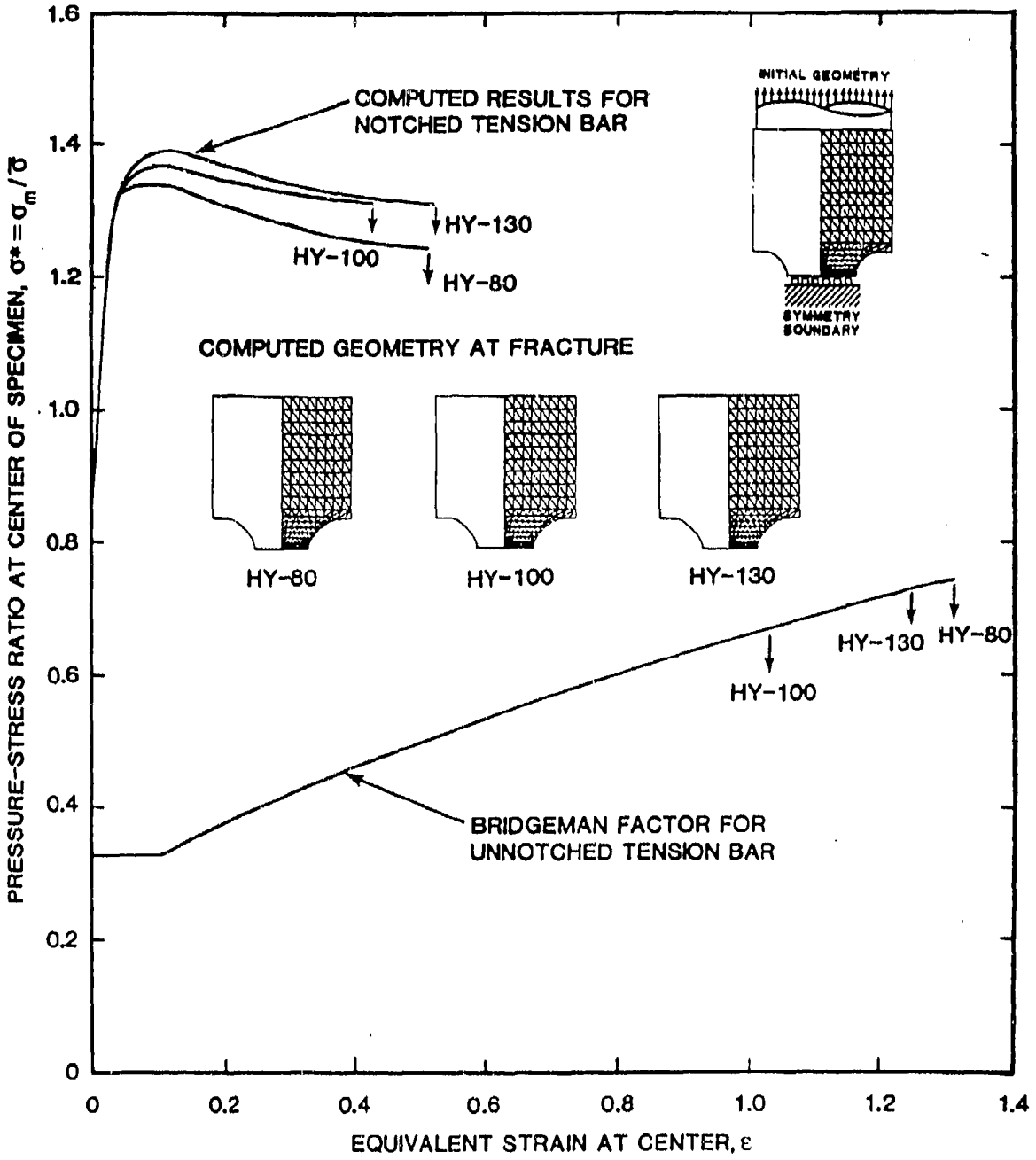

FIGURE 18. PRESSURE-STRESS RATIO VERSUS EQUIVALENT STRAIN FOR THE TENSILE SPECIMENS

For the notched tensions bars, the computed pressure-stress ratio begins at approximately $\sigma^* = 0.8$ and peaks somewhere between $\sigma^* = 1.3$ to 1.4, depending on the material. After its peak the pressure-stress ratio gradually decreases until fracture. It should be noted that each curve's maximum pressure-stress ratio is in the same order as their respective strengths.

Figure 19 shows the equivalent plastic strain to fracture as a function of the pressure-stress ratio for quasi-static conditions. For all three materials an approximate analytic fit to the data was performed by setting D3 = -0.5, and solving for D1 and D2.

Figure 20 shows the effect of strain rate and temperature on the strain to fracture. The fracture strains are expressed as the ratio of the Hopkinson bar fracture strains divided by the quasi-static tensile fracture strains. The Hopkinson bar fracture strains are approximately determined by measuring the cross-sectional area of the post-tested specimens as shown in Figures 7 to 9. Unfortunately, these areas cannot be measured with a high degree of accuracy. The temperatures for each test range from the initial temperature at the beginning of the test to the computed temperature at the strain where fracture occurs.

For example, in Figure 20, for the first test performed on the HY-100 material the specimen was initially at room temperature ($T^* = 0$). If all the plastic work is converted to adiabatic heat, the computed final temperature is 606K ($T^* = .21$). The strain at which this specimen fractured was $\varepsilon_f = 1.13$, at an average strain rate of $\dot{\varepsilon} \approx 550s^{-1}$. The quasi-static ($\dot{\varepsilon} \approx .002s^{-1}$), room temperature ($T^* = 0$) tension test is used as the normalizing denominator for the vertical axis. For the HY-100 material this fracture strain is $\varepsilon_f = 1.04$. The ratio of these two fractures strains is 1.09 and is the value plotted on the vertical axis. The same procedure is used for the remaining three HY-100 tests with the only difference being the initial temperature of the specimen.

Under normal conditions a linear least squares fit is performed on the data of each material in Figure 20, of which the intercept is the strain rate influence on fracture and the slope is the temperature influence. The HY-80, HY-100, and HY-130 materials acted differently than expected, displaying a consistent trend of reaching a peak fracture strain ratio between .15T* and .35T* and then becoming less ductile as the temperature is increased (Figure 20). Possible explanations for this behavior is that the material becomes strain rate sensitive at higher temperatures as shown in Figure 17, or it may be experiencing a phenomena referred to as 'temper embrittlement' where under certain tempering processes a metal becomes less ductile.

The current fracture model was not developed to handle the phenomena which is occurring with the HY materials. By applying the linear least squares fit to the data, one obtains deceiving results, implying that the material is very strain rate sensitive and loses ductility as the temperature increases. A more realistic approach to incorporate this data into the fracture model is to obtain an 'average' strain rate constant and neglect thermal effects. In graphical terms, fit the best horizontal line to the data points of each material as shown on the right hand side in Figure 20.

Now the fracture constants can be determined. The strain rate constant, D4, is obtained by averaging the fracture strain ratios of Figure 20 for each respective material. The average strain rate constant for all three is greater than 1.0. This

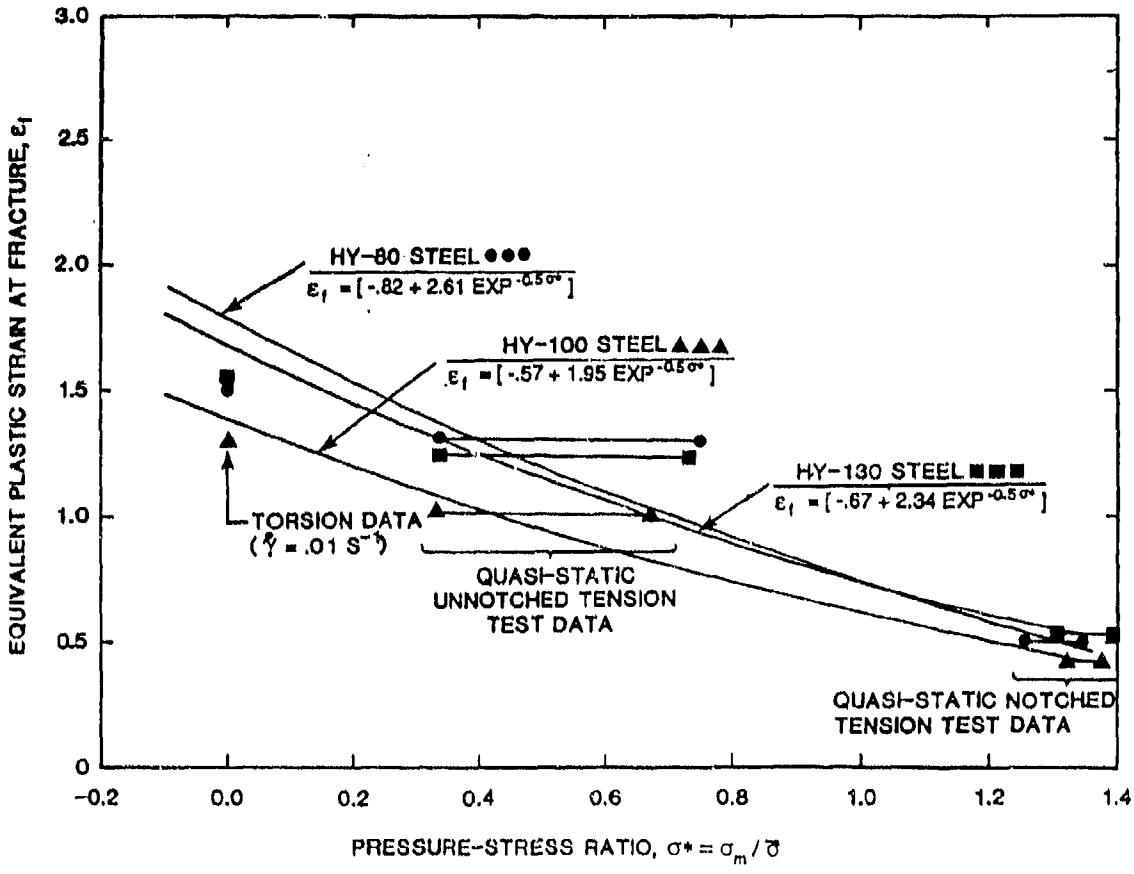

FIGURE 19. FRACTURE STRAIN VERSUS PRESSURE-STRESS RATIO FOR ISOTHERMAL QUASI-STATIC CONDITIONS

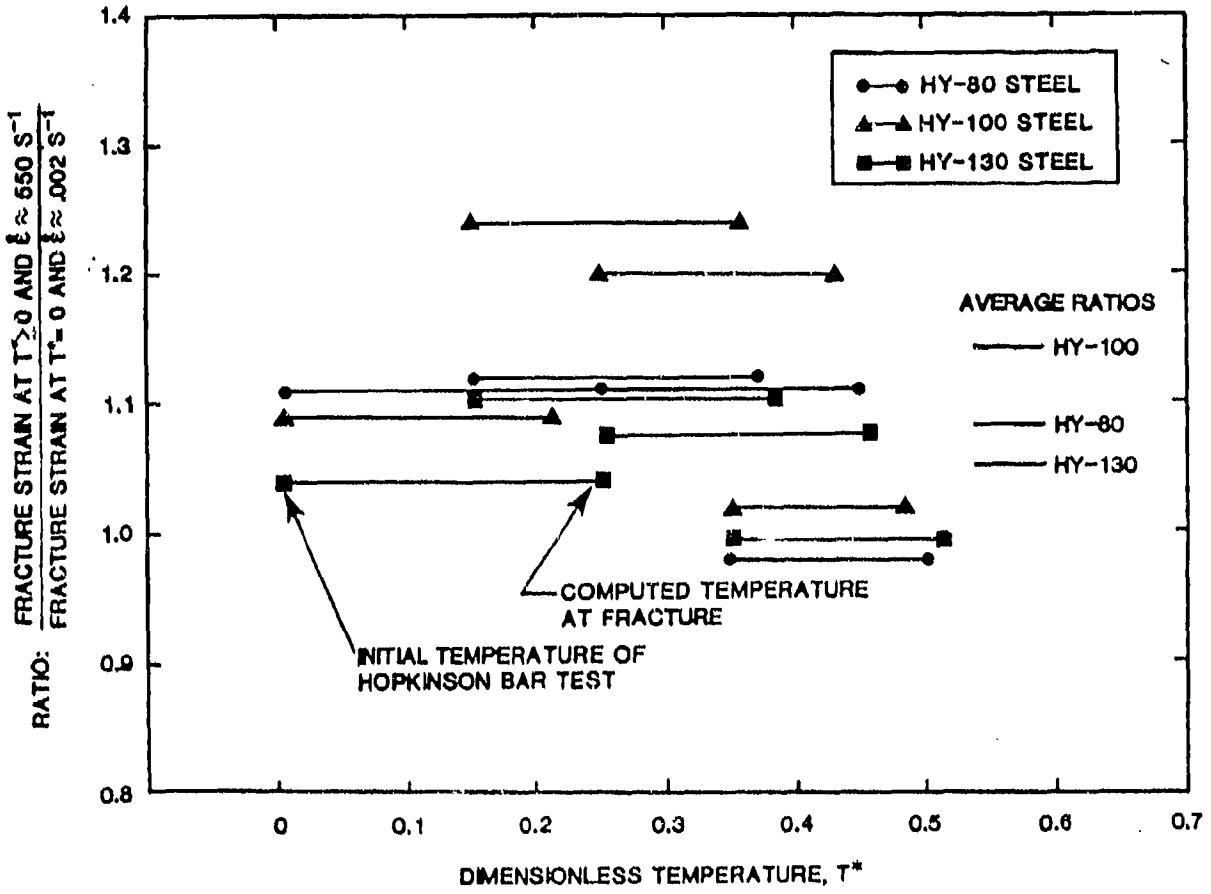

FIGURE 20. EFFECTS OF STRAIN RATE AND TEMPERATURE ON FRACTURE STRAINS

ratio indicates that the strain to fracture increases slightly as the strain rate increases. This same trend is verified by the fracture data of Figure 17. (The decrease in fracture strains for the higher strain rate torsion data may be due to shear localizations resulting from adiabatic heating.[4,5]) The constants related to the pressure-stress ratio (D1, D2, D3) are those of Figure 19, adjusted from quasi-static conditions ($\dot{\varepsilon} = .002s^{-1}$) to $\varepsilon^* = 1.0$. Finally, the temperature constant, D5, is set to zero, due to the unconforming data of Figure 20. The resulting relationships are shown in Figures 21 to 23.

Unlike the strength relationships, which transitioned in a well-behaved manner from HY-80 to HY-130, the fracture characteristics do not follow a well-behaved pattern. The HY-80 steel exhibits the most ductility, as expected, but the HY-100 is the least ductile. Generally, it would be expected that the higher strength HY-130 steel would exhibit less ductility. The reasons for this apparent discrepancy are not clear.

Although no tests were performed to obtain spall characteristics of HY-80, HY-100, and HY-130, it is necessary to designate a spall stress and strain to complete the model. Based on comparisons with materials of similar yield strengths, the spall stress and strain were estimated and are shown in Table 2.

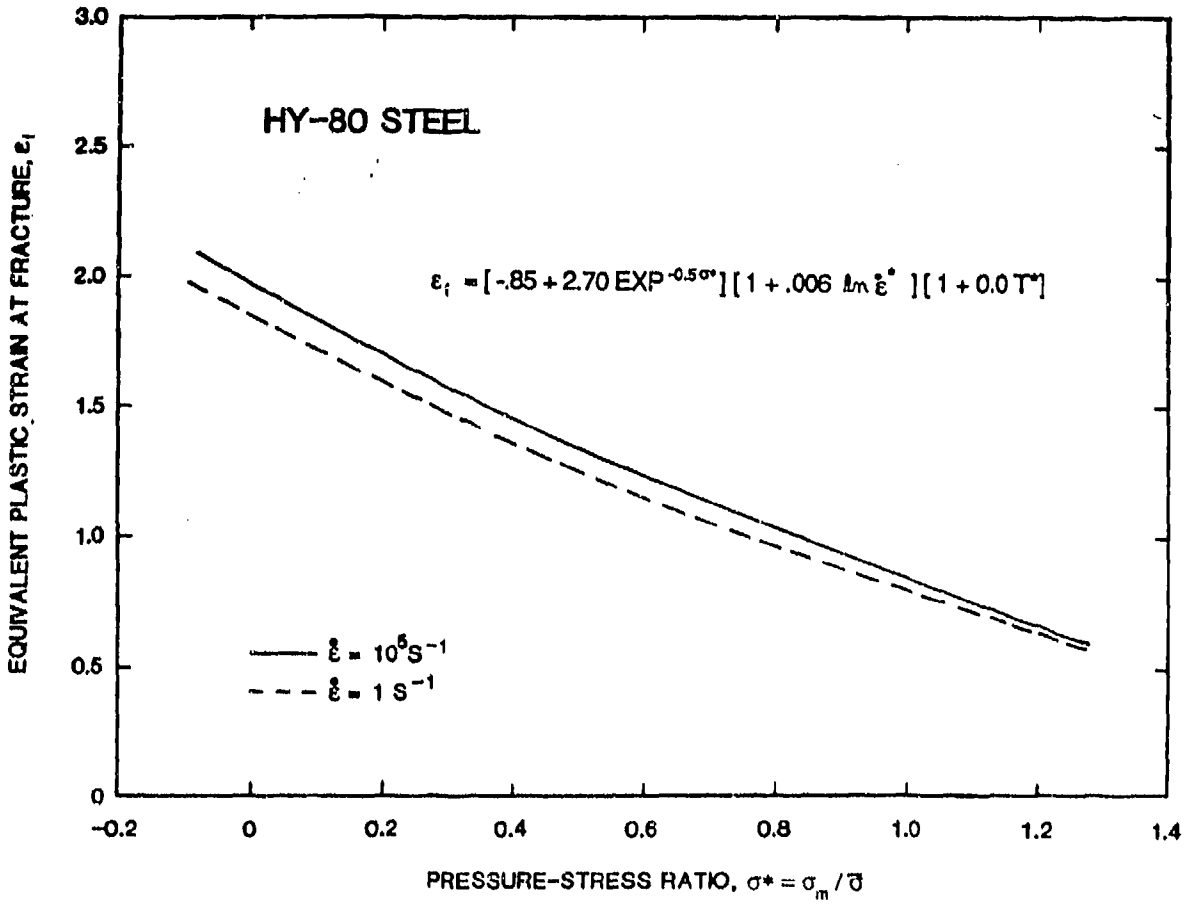

FIGURE 21. FRACTURE STRAIN AS A FUNCTION OF PRESSURE-STRESS RATIO, STRAIN RATE, AND TEMPERATURE FOR HY-80 STEEL

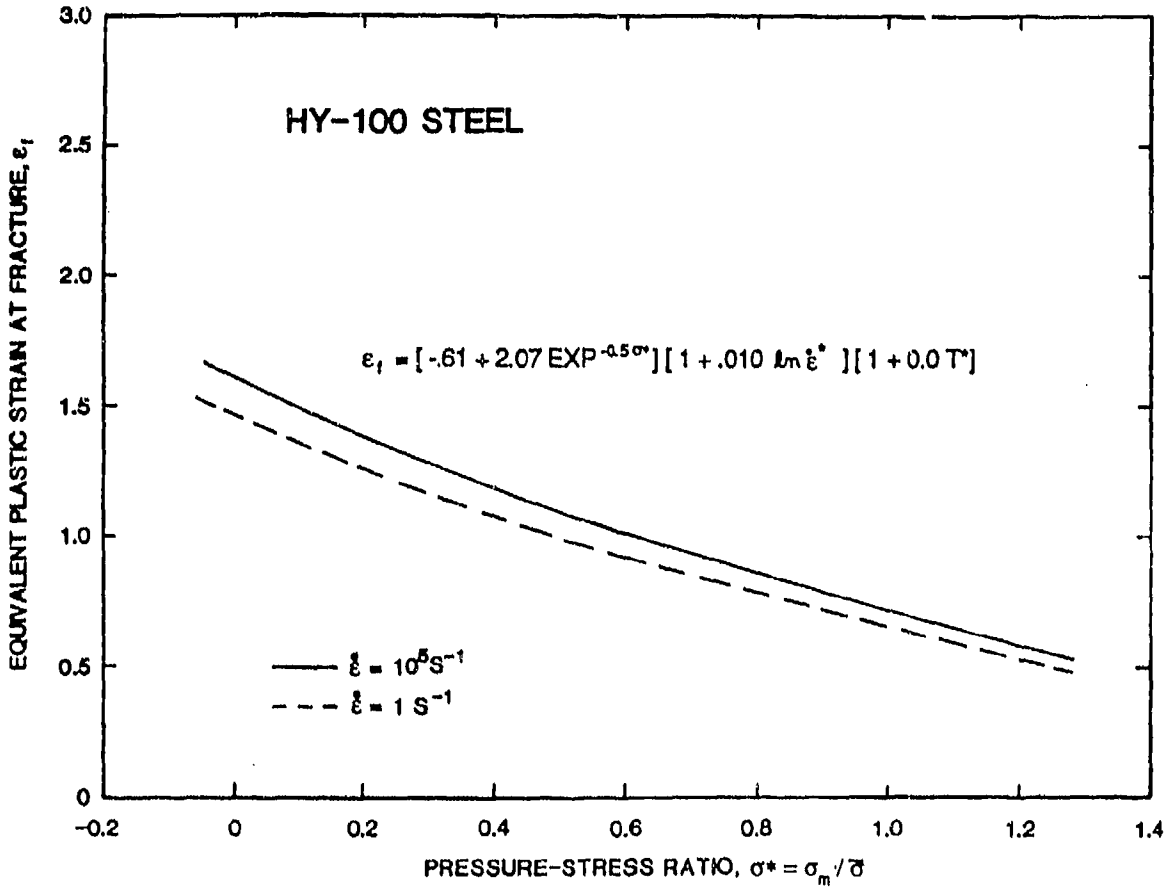

FIGURE 22. FRACTURE STRAIN AS A FUNCTION OF PRESSURE-STRESS RATIO, STRAIN RATE, AND TEMPERATURE FOR HY-100 STEEL

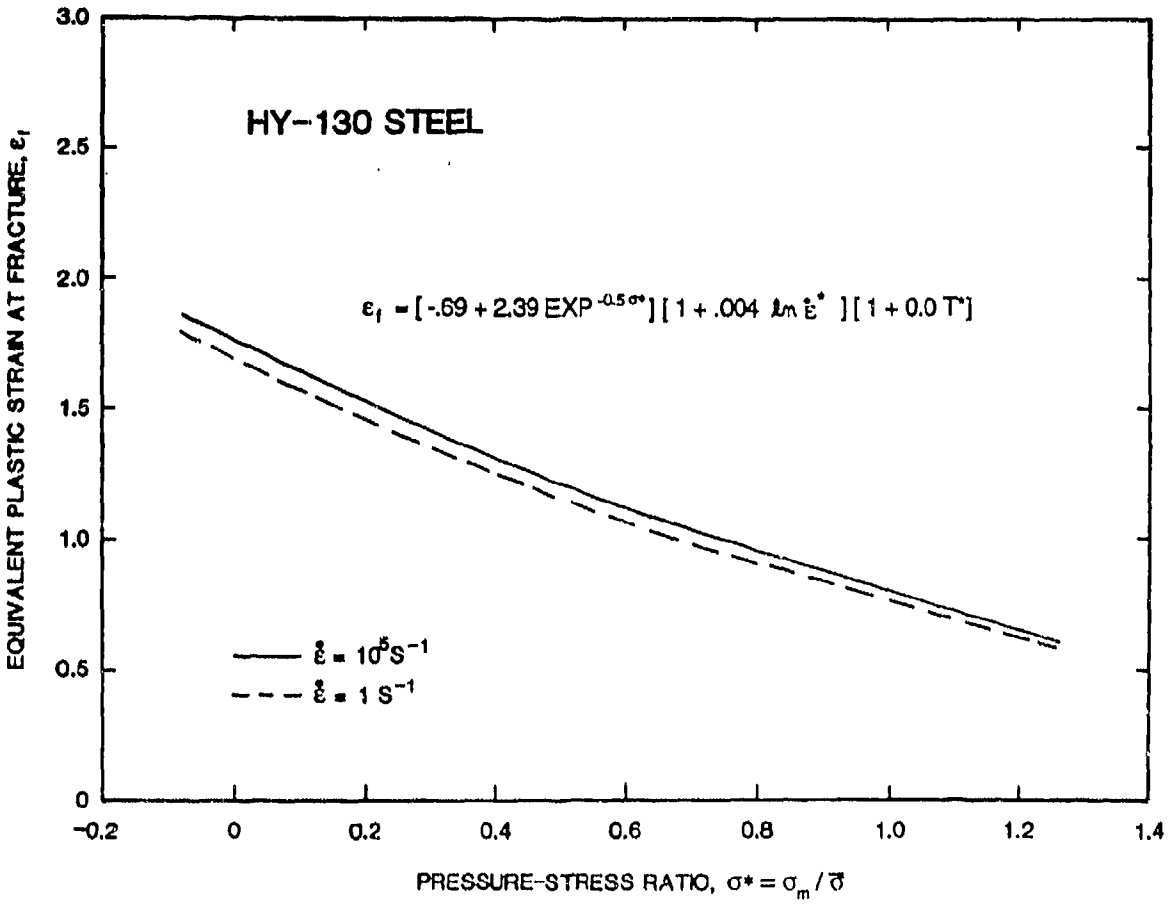

FIGURE 23. FRACTURE STRAIN AS A FUNCTION OF PRESSURE-STRESS RATIO, STRAIN RATE, AND TEMPERATURE FOR HY-130 STEEL

TABLE 2. SUMMARY OF STRENGTH AND FRACTURE MODEL CONSTANTS FOR HY-80, HY-100, AND HY-130 STEEL

		HY-80 STEEL	HY-100 STEEL	HY-130 STEEL
STRENGTH CONSTANTS FOR $\sigma = [A + B\varepsilon^n][1 + C \ln \dot{\varepsilon}^*][1 - T^{*m}]$				
A	(MPa)	672	758	920
B	(MPa)	425	402	333
n		.36	.26	.39
C		.014	.011	.008
m		1.14	1.13	1.15
FRACTURE CONSTANTS FOR $\varepsilon_f = [D_1 + D_2 \text{EXP } D_3\sigma^*][1 + D_4 \ln \dot{\varepsilon}^*][1 + D_5 T^*]$				
D_1		-.85	-.61	-.69
D_2		2.70	2.07	2.39
D_3		-0.50	-0.50	-0.50
D_4		.006	.010	.004
D_5		0.0	0.0	0.0
SPALL STRESS, σ_{SPALL}	(MPa)	5500	5600	5900
ε_f^{min}		.033	.034	.036
$\sigma^* = \sigma_m/\bar{\sigma}$				
$\dot{\varepsilon}^* = \dot{\varepsilon}/\dot{\varepsilon}_0$ FOR $\dot{\varepsilon}_0 = 1.0\ S^{-1}$				
$T^* = (T - T_{ROOM})/(T_{MELT} - T_{ROOM})$				

N07-021.JF

SECTION 5

CONSTANTS FOR EPIC-2/EPIC-3 DATA LIBRARY

A summary of the strength and fracture model constants is given in Table 2. Data statements for the EPIC-2/EPIC-3 material library (Subroutine MATLIB) are shown in Figure 24, and the corresponding Preprocessor output is shown in Figures 25 to 27.

```
C
C *** HY-80 STEEL ************************************** TJH - AUG 1987
C *** LIMITED TO U.S. GOVERNMENT AGENCIES ONLY
C     PRESSURE - KOHN, AFWL-TR-69-38, 1969, P. 140 (STAINLESS STEEL 304L)
C     STRENGTH - HOLMQUIST, NSWC REPORT 1987
C     FRACTURE - HOLMQUIST, NSWC REPORT 1987
C     SPALL    - OVERESTIMATED FROM DATA IN AFWAL-TR-81-4040, 1981
      DATA MTYPE(25)/1/,IDAM(25)/0/,IFAIL(25)/0/,EFAIL(25)/999./,
     1     DEN(25)/.000725/,SPH(25)/433000./,CDUCT(25)/4.32/,
     2     ALPHA(25)/.0000063/,TEMP1(25)/70./,TROOM(25)/70./,
     3     TMELT(25)/2768./,C8(25)/.02/,G(25)/11240000./,
     4     C1(25)/97460./,C2(25)/61640./,AN(25)/.36/,C3(25)/.014/,
     5     AM(25)/1.14/,C4(25)/0./,C5(25)/0./,C(25)/23776000./,
     6     D(25)/42693000./,S(25)/72513000./,GRUN(25)/1.16/,
     7     Q1(25)/.2/,Q2(25)/4./,PMIN(25)/10000000./,C9(25)/0./,
     8     D1(25)/-.85/,D2(25)/2.70/,D3(25)/-.50/,D4(25)/.006/,
     9     D5(25)/0.00/,PFAIL(25)/795000./,EFMIN(25)/.033/,C10(25)/0./,
     A     (DESCM(25,J),J=1,4) /4H*HY-,4H80 S,4HTEEL,4H    /,
     B     (DESCM(25,J),J=5,8) /4H    ,4H    ,4HRC-2,4H1   /,
     C     (DESCM(25,J),J=9,12)/4H    ,4H    ,4H    ,4H    /

C
C *** HY-100 STEEL ************************************* TJH - AUG 1987
C *** LIMITED TO U.S. GOVERNMENT AGENCIES ONLY
C     PRESSURE - KOHN, AFWL-TR-69-38, 1969, P. 140 (STAINLESS STEEL 304L)
C     STRENGTH - HOLMQUIST, NSWC REPORT 1987
C     FRACTURE - HOLMQUIST, NSWC REPORT 1987
C     SPALL    - OVERESTIMATED FROM DATA IN AFWAL-TR-81-4040, 1981
      DATA MTYPE(26)/1/,IDAM(26)/0/,IFAIL(26)/0/,EFAIL(26)/999./,
     1     DEN(26)/.000725/,SPH(26)/433000./,CDUCT(26)/4.32/,
     2     ALPHA(26)/.0000077/,TEMP1(26)/70./,TROOM(26)/70./,
     3     TMELT(26)/2768./,C8(26)/.02/,G(26)/11240000./,
     4     C1(26)/109900./,C2(26)/58300./,AN(26)/.26/,C3(26)/.011/,
     5     AM(26)/1.13/,C4(26)/0./,C5(26)/0./,C(26)/23776000./,
     6     D(26)/42693000./,S(26)/72513000./,GRUN(26)/1.16/,
     7     Q1(26)/.2/,Q2(26)/4./,PMIN(26)/10000000./,C9(26)/0./,
     8     D1(26)/-.61/,D2(26)/2.07/,D3(26)/-.50/,D4(26)/.010/,
     9     D5(26)/0.00/,PFAIL(26)/819300./,EFMIN(26)/.034/,C10(26)/0./,
     A     (DESCM(26,J),J=1,4) /4H*HY-,4H100 ,4HSTEE,4HL   /,
     B     (DESCM(26,J),J=5,8) /4H    ,4H    ,4HRC-2,4H5   /,
     C     (DESCM(26,J),J=9,12)/4H    ,4H    ,4H    ,4H    /

C
C *** HY-130 STEEL ************************************* TJH - AUG 1987
C *** LIMITED TO U.S. GOVERNMENT AGENCIES ONLY
C     PRESSURE - KOHN, AFWL-TR-69-38, 1969, P. 140 (STAINLESS STEEL 304L)
C     STRENGTH - HOLMQUIST, NSWC REPORT 1987
C     FRACTURE - HOLMQUIST, NSWC REPORT 1987
C     SPALL    - OVERESTIMATED FROM DATA IN AFWAL-TR-81-4040, 1981
      DATA MTYPE(27)/1/,IDAM(27)/0/,IFAIL(27)/0/,EFAIL(27)/999./,
     1     DEN(27)/.000738/,SPH(27)/422000./,CDUCT(27)/3.46/,
     2     ALPHA(27)/.0000073/,TEMP1(27)/70./,TROOM(27)/70./,
     3     TMELT(27)/2768./,C8(27)/.02/,G(27)/11240000./,
     4     C1(27)/133400./,C2(27)/48300./,AN(27)/.39/,C3(27)/.008/,
     5     AM(27)/1.15/,C4(27)/0./,C5(27)/0./,C(27)/23776000./,
     6     D(27)/42693000./,S(27)/72513000./,GRUN(27)/1.16/,
     7     Q1(27)/.2/,Q2(27)/4./,PMIN(27)/10000000./,C9(27)/0./,
     8     D1(27)/-.69/,D2(27)/2.39/,D3(27)/-.50/,D4(27)/.004/,
     9     D5(27)/0.00/,PFAIL(27)/860000./,EFMIN(27)/.036/,C10(27)/0./,
     A     (DESCM(27,J),J=1,4) /4H*HY-,4H130 ,4HSTEE,4HL   /,
     B     (DESCM(27,J),J=5,8) /4H    ,4H    ,4HRC-3,4H0   /,
     C     (DESCM(27,J),J=9,12)/4H    ,4H    ,4H    ,4H    /
```

FIGURE 24. DATA STATEMENTS FOR THE EPIC-2/EPIC-3 MATERIAL LIBRARY IN ENGLISH UNITS

```
INPUT DATA FOR SOLID MATERIAL

MATERIAL NUMBER   25      *HY-80 STEEL                RC-21


MASS/THERMAL PROPERTIES
  DENSITY                      =     0.725000E-03
  SPECIFIC HEAT                =     0.433000E+06
  CONDUCTIVITY                 =     0.432000E+01
  VOLUME EXPANSION COEF        =     0.630000E-05
  INITIAL TEMPERATURE          =     0.700000E+02
  ROOM TEMPERATURE             =     0.700000E+02
  MELTING TEMPERATURE          =     0.276800E+04
STRENGTH PROPERTIES
  SHEAR MODULUS                =     0.112400E+08
  YIELD STRESS, C1             =     0.974600E+05
  HARDENING COEF, C2           =     0.616400E+05
  HARDENING EXPONENT, N        =     0.360000E+00
  STRAIN RATE COEF, C3         =     0.140000E-01
  SOFTENING EXPONENT, M        =     0.114000E+01
  PRESSURE COEF, C4            =     0.000000E+00
  MAX STRENGTH (OPTIONAL)      =     0.000000E+00
EQUATION OF STATE
  K1                           =     0.237760E+08
  K2                           =     0.426930E+08
  K3                           =     0.725130E+08
  GRUNEISEN COEF               =     0.116000E+01
  MAX NEGATIVE PRESSURE        =     0.100000E+08
ARTIFICIAL VISCOSITY
  LINEAR COEF                  =     0.200000E+00
  QUADRATIC COEF               =     0.400000E+01
  HOURGLASS COEF               =     0.200000E-01
FRACTURE PROPERTIES
  DAMAGE COMPUTED              =       0
  FRACTURE ALLOWED             =       0
  D1                           =    -0.850000E+00
  D2                           =     0.270000E+01
  D3                           =    -0.500000E+00
  D4                           =     0.600000E-02
  D5                           =     0.000000E+00
  MINIMUM FRACTURE STRAIN      =     0.330000E-01
  SPALL STRENGTH               =     0.795000E+06
  STRAIN FOR TOTAL FAILURE     =     0.999000E+03
EXTRA CONSTANTS
  X1 (C9) CERAMICS CRUSHED     =     0.000000E+00
  X2 (C10)                     =     0.000000E+00
```

FIGURE 25. EPIC-2/EPIC-3 PREPROCESSOR OUTPUT FOR THE MATERIAL DATA IN ENGLISH UNITS FOR HY-80 STEEL

```
INPUT DATA FOR SOLID MATERIAL

MATERIAL NUMBER   26      *HY-100 STEEL              RC-25


MASS/THERMAL PROPERTIES
  DENSITY                      =    0.725000E-03
  SPECIFIC HEAT                =    0.433000E+06
  CONDUCTIVITY                 =    0.432000E+01
  VOLUME EXPANSION COEF        =    0.770000E-05
  INITIAL TEMPERATURE          =    0.700000E+02
  ROOM TEMPERATURE             =    0.700000E+02
  MELTING TEMPERATURE          =    0.276800E+04
STRENGTH PROPERTIES
  SHEAR MODULUS                =    0.112400E+08
  YIELD STRESS, C1             =    0.109900E+06
  HARDENING COEF, C2           =    0.583000E+05
  HARDENING EXPONENT, N        =    0.260000E+00
  STRAIN RATE COEF, C3         =    0.110000E-01
  SOFTENING EXPONENT, M        =    0.113000E+01
  PRESSURE COEF, C4            =    0.000000E+00
  MAX STRENGTH (OPTIONAL)      =    0.000000E+00
EQUATION OF STATE
  K1                           =    0.237760E+08
  K2                           =    0.426930E+08
  K3                           =    0.725130E+08
  GRUNEISEN COEF               =    0.116000E+01
  MAX NEGATIVE PRESSURE        =    0.100000E+08
ARTIFICIAL VISCOSITY
  LINEAR COEF                  =    0.200000E+00
  QUADRATIC COEF               =    0.400000E+01
  HOURGLASS COEF               =    0.200000E-01
FRACTURE PROPERTIES
  DAMAGE COMPUTED              =    0
  FRACTURE ALLOWED             =    0
  D1                           =   -0.610000E+00
  D2                           =    0.207000E+01
  D3                           =   -0.500000E+00
  D4                           =    0.100000E-01
  D5                           =    0.000000E+00
  MINIMUM FRACTURE STRAIN      =    0.340000E-01
  SPALL STRENGTH               =    0.819300E+06
  STRAIN FOR TOTAL FAILURE     =    0.999000E+03
EXTRA CONSTANTS
  X1 (C9) CERAMICS CRUSHED     =    0.000000E+00
  X2 (C10)                     =    0.000000E+00
```

FIGURE 26. EPIC-2/EPIC-3 PREPROCESSOR OUTPUT FOR THE MATERIAL DATA IN ENGLISH UNITS FOR HY-100 STEEL

```
INPUT DATA FOR SOLID MATERIAL

MATERIAL NUMBER   27      *HY-130 STEEL              RC-30


MASS/THERMAL PROPERTIES
  DENSITY                      =    0.738000E-03
  SPECIFIC HEAT                =    0.422000E+06
  CONDUCTIVITY                 =    0.346000E+01
  VOLUME EXPANSION COEF        =    0.730000E-05
  INITIAL TEMPERATURE          =    0.700000E+02
  ROOM TEMPERATURE             =    0.700000E+02
  MELTING TEMPERATURE          =    0.276800E+04
STRENGTH PROPERTIES
  SHEAR MODULUS                =    0.112400E+08
  YIELD STRESS, C1             =    0.133400E+06
  HARDENING COEF, C2           =    0.483000E+05
  HARDENING EXPONENT, N        =    0.390000E+00
  STRAIN RATE COEF, C3         =    0.800000E-02
  SOFTENING EXPONENT, M        =    0.115000E+01
  PRESSURE COEF, C4            =    0.000000E+00
  MAX STRENGTH (OPTIONAL)      =    0.000000E+00
EQUATION OF STATE
  K1                           =    0.237760E+08
  K2                           =    0.426930E+08
  K3                           =    0.725130E+08
  GRUNEISEN COEF               =    0.116000E+01
  MAX NEGATIVE PRESSURE        =    0.100000E+08
ARTIFICIAL VISCOSITY
  LINEAR COEF                  =    0.200000E+00
  QUADRATIC COEF               =    0.400000E+01
  HOURGLASS COEF               =    0.200000E-01
FRACTURE PROPERTIES
  DAMAGE COMPUTED              =    0
  FRACTURE ALLOWED             =    0
  D1                           =   -0.690000E+00
  D2                           =    0.239000E+01
  D3                           =   -0.500000E+00
  D4                           =    0.400000E-02
  D5                           =    0.000000E+00
  MINIMUM FRACTURE STRAIN      =    0.360000E-01
  SPALL STRENGTH               =    0.860000E+06
  STRAIN FOR TOTAL FAILURE     =    0.999000E+03
EXTRA CONSTANTS
  X1 (C9) CERAMICS CRUSHED     =    0.000000E+00
  X2 (C10)                     =    0.000000E+00
```

FIGURE 27. EPIC-2/EPIC-3 PREPROCESSOR OUTPUT FOR THE MATERIAL DATA IN ENGLISH UNITS FOR HY-130 STEEL

SECTION 6

SUMMARY

HY-80, HY-100, and HY-130 steels have been tested at various strains, strain rates, temperatures and pressure. The results of these have been analyzed to obtain strength and fracture constants for the corresponding models in the EPIC-2/EPIC-3 codes. These constants have been incorporated into the EPIC-2/EPIC-3 material data library.

REFERENCES

1. Johnson, G.R. and Stryk, R.A., User Instructions for the EPIC-2 Code, AFATL-TR-86-51, Honeywell Inc., Defense Systems Division, Edina, MN, Sep 1986.

2. Johnson, G.R. and Stryk, R.A., User Instructions for the EPIC-3 Code, AFATL-TR-87-10, Honeywell Inc., Defense Systems Division, Brooklyn Park, MN, May 1987.

3. Alloy Digest, Published by Engineering Alloys Digest, Inc., Upper Montclair, NJ, Aug 1970.

4. Johnson, G.R., Hoegfeldt, J.M., Lindholm, U.S., and Nagy, A., "Response of Various Metals to Large Torsional Strains Over A Large Range of Strain Rates - Part 1: Ductile Metals," ASME Journal of Engineering Materials and Technology, Vol. 105, No. 1, Jan 1983, p. 42.

5. Johnson, G.R., Hoegfeldt, J.M., Lindholm, U.S., and Nagy, A., "Response of Various Metals to Large Torsional Strains Over a Large Range of Strain Rates - Part 2: Less Ductile Metals," ASME Journal of Engineering Materials and Technology, Vol 105, No. 1, Jan 1983, p. 48.

6. Mackenzie, A.C., Hancock, J.W., and Brown, D.K., "On the Influence of State Stress on Ductile Failure Initiation in High Strength Steels," Engineering Fracture Mechanics, Vol. 9, 1977, p. 167.

7. Johnson, G.R., Development of Strength and Fracture Models for Computations Involving Severe Dynamic Loading - Volume I: Strength and Fracture Models, AFATL-TR-83-05, Honeywell Inc., Defense Systems Division, Edina, MN, Jan 1986.

8. Johnson, G.R. and Cook, W.H., "A Constitutive Model and Data for Metals Subjected to Large Strains, High Strain Rates and High Temperatures," Proceedings of Seventh International Symposium on Ballistics, The Hague, The Netherlands, Apr 1983.

9. Johnson, G.R. and Cook, W.H., "Fracture Characteristics of Three Metals Subjected to Various Strains, Strain Rates, Temperatures and Pressures," Journal of Engineering Fracture Mechanics, Vol. 21, No. 1, 1985, p. 31.

10. Hancock, J.W. and Mackenzie, A.C., "On the Mechanism of Ductile Failure in High-Strength Steels Subjected to Multi-Axial Stress-States," Journal of Mechanics and Physics of Solids, Jun 1976, p. 147.

REFERENCES (Cont.)

11. Nagtegaal, J.C., Parks, D.M., and Rice, J.R., "On Numerically Accurate Finite Element Solutions in Fully Plastic Range," Computer Methods in Mechanics and Engineering, Vol. 4, 1974, p. 153.

APPENDIX A

METALLURGICAL RESULTS OF HY-80, HY-100, AND HY-130 STEEL

The metallugrical samples of each material were prepared in cross section for examination in three planes using an autopolishing technique and etched with 3 percent nital. The three orientations examined were: a plane parallel to the plate surface and two planes 90° to each other viewing the plate cross section. Various degrees of typical inclusions were noted in the fine tempered martensitic structures. The HY-130 (higher strength material) exhibited only spot, no linear inclusions. Tyoical microstructures are illustrated: HY-80, Figures A-1 to A-5; HY-100, Figures A-6 to A-10; and HY-130, Figures A-11 to A-14.

Honeywell

DEFENSE SYSTEMS DIVISION
MATERIALS AND PROCESS ENGINEERING

ETR NUMBER 6014

VIEW A
MAGNIFICATION: 200X

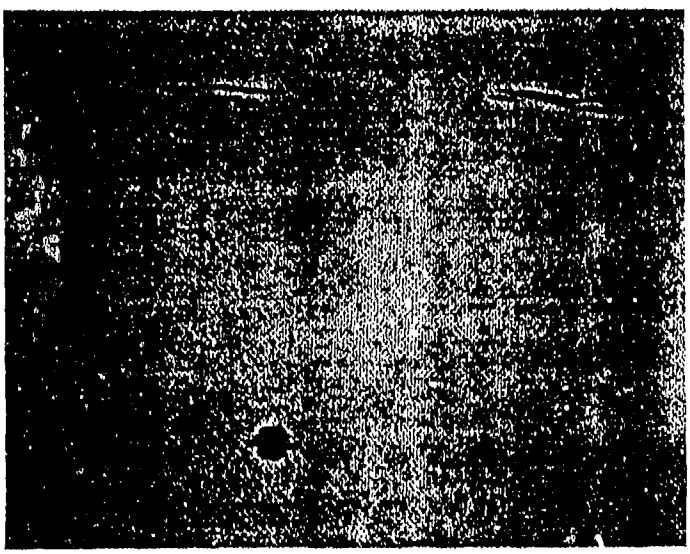

VIEW B
MAGNIFICATION: 500X

FIGURE	M & PE LAB NUMBER	M & PE ENGINEER	M & PE TECHNICIAN	DEVICE/PART NUMBER
A-1	27478		D. Dehmer	HY-80 Steel

Photomicrographs of HY80 steel in cross section at various magnifications, viewing a plane perpendicular to the sample length. Views A and B illustrate typical inclusions prior to etching. Etchant: 3% nital.

HP 532 REV 1/86

Honeywell

DEFENSE SYSTEMS DIVISION
MATERIALS AND PROCESS ENGINEERING

ETR NUMBER 6014

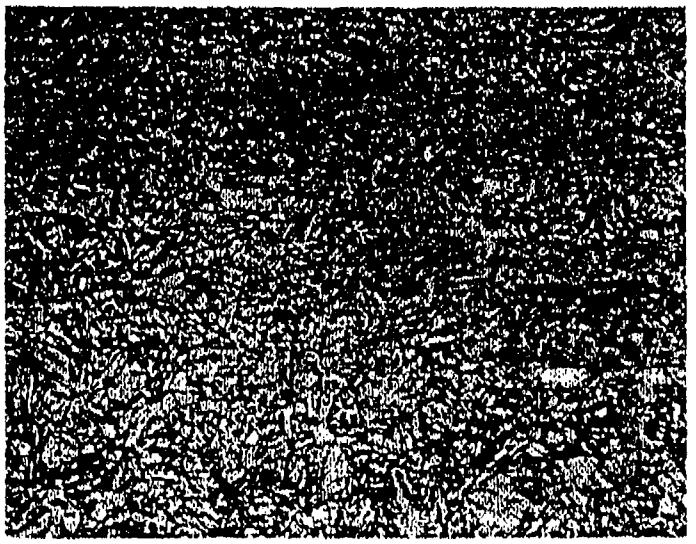

VIEW A
MAGNIFICATION: 200X

VIEW B
MAGNIFICATION: 500X

FIGURE	M & PE LAB NUMBER	M & PE ENGINEER	M & PE TECHNICIAN	DEVICE PART NUMBER
A-2	27478		D. Dahmer	HY-80 Steel

Microstructure photomicrographs of HY80 steel in cross section at various magnifications, viewing a plane parallel to the sample length. Views A & B illustrate typical inclusions following etching. Etchant: 3% nital.

HP 532 REV 1-86

Honeywell

DEFENSE SYSTEMS DIVISION
MATERIALS AND PROCESS ENGINEERING

ETR NUMBER 6014

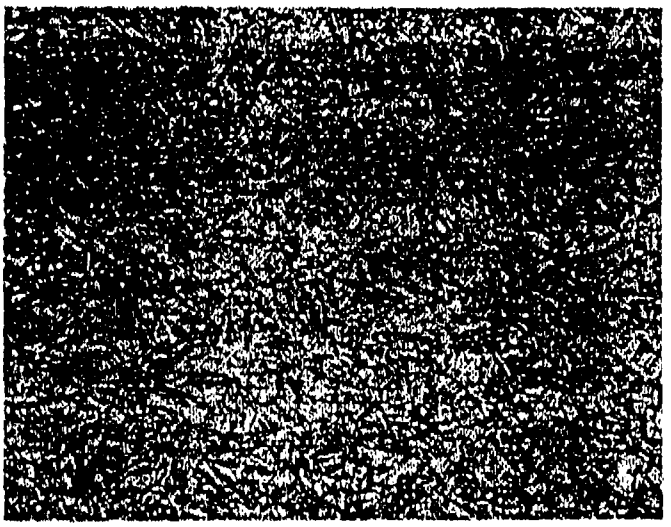

VIEW A
MAGNIFICATION: 200X

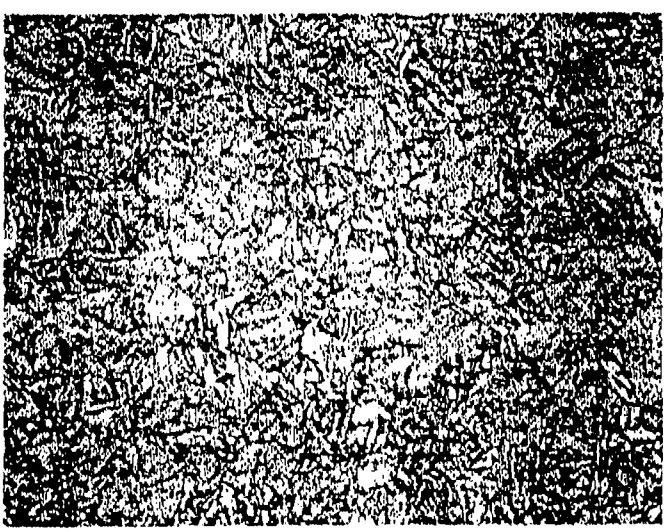

VIEW B
MAGNIFICATION: 500X

FIGURE	M & PE LAB NUMBER	M & PE ENGINEER	M & PE TECHNICIAN	DEVICE/PART NUMBER
A-3	27478		D. Dehmer	HY-80 Steel

Microstructure photomicrographs of HY80 steel in cross section at various magnifications, viewing a plane parallel to the plate surface. Views A & B illustrate tempered martensite. Etchant: 3% nital.

HP 5.32 REV 1 86

Honeywell

DEFENSE SYSTEMS DIVISION
MATERIALS AND PROCESS ENGINEERING

ETR NUMBER 6014

VIEW A
MAGNIFICATION: 200X

VIEW B
MAGNIFICATION: 500X

FIGURE	M & PE LAB NUMBER	M & PE ENGINEER	M & PE TECHNICIAN	DEVICE/PART NUMBER
A-4	27478		D. Dohmer	HY-80 Steel

Microstructure photomicrographs of HY80 steel in cross section at various magnifications, viewing a plane parallel to the sample length. Views A & B illustrate tempered martensite. Etchant: 3% nital.

HP-532 REV 1/88

Honeywell

DEFENSE SYSTEMS DIVISION
MATERIALS AND PROCESS ENGINEERING

ETR NUMBER 6014

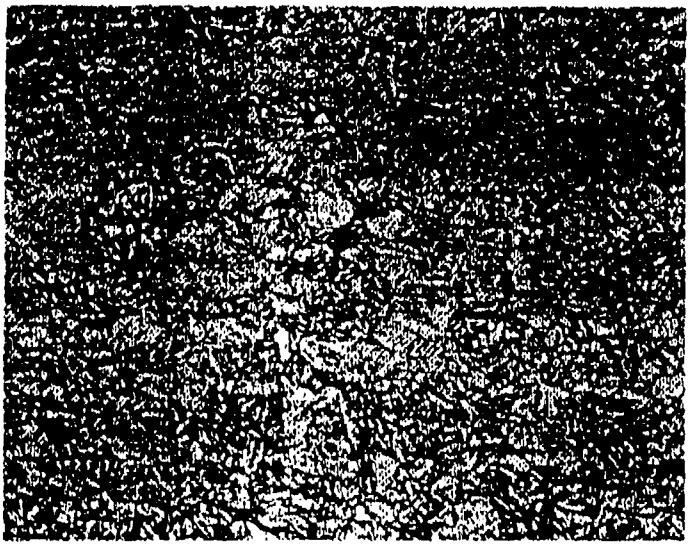

VIEW A
MAGNIFICATION: 200X

VIEW B
MAGNIFICATION: 500X

FIGURE	M & PE LAB NUMBER	M & PE ENGINEER	M & PE TECHNICIAN	DEVICE/PART NUMBER
A-5	27478		D. Dehmer	HY-80 Steel

Microstructure photomicrographs of HY80 steel in cross section at various magnifications, viewing a plane perpendicular to the sample length. Views A & B illustrate tempered martensite. Etchant: 3% nital.

HP-632 REV 1/86

Honeywell

DEFENSE SYSTEMS DIVISION
MATERIALS AND PROCESS ENGINEERING

ETR NUMBER 6014

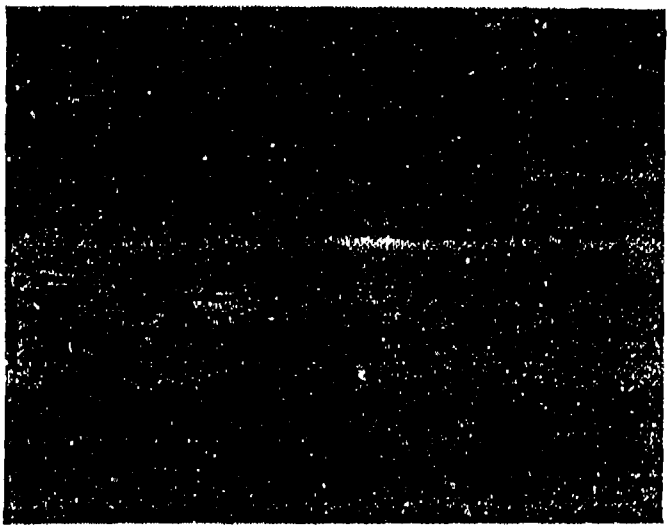

VIEW A
MAGNIFICATION: 200X

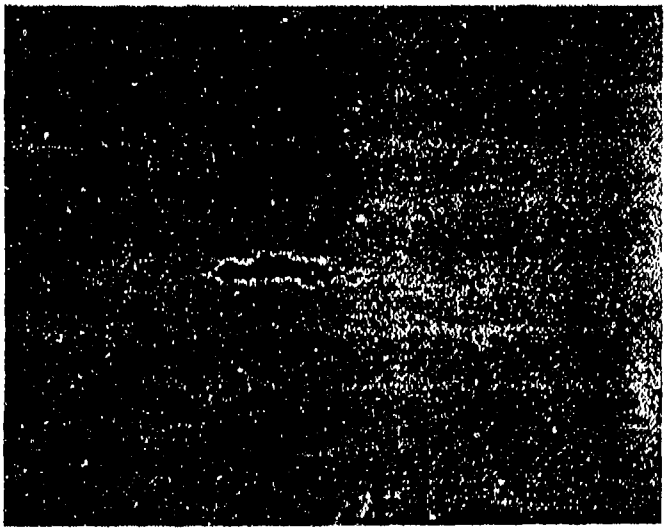

VIEW B
MAGNIFICATION: 200X

FIGURE	M & PE LAB NUMBER	M & PE ENGINEER	M & PE TECHNICIAN	DEVICE/PART NUMBER
A-6	27478		D. Dehmer	HY-100 Steel

Photomicrographs of HY100 steel in cross section, viewing a plane parallel to the sample length. Views A & B illustrate an inclusion at the surface continuing in the plate prior to etching. Etchant: 3% nital

HP 532 REV 1-86

Honeywell

DEFENSE SYSTEMS DIVISION
MATERIALS AND PROCESS ENGINEEPING

ETR NUMBER 6014

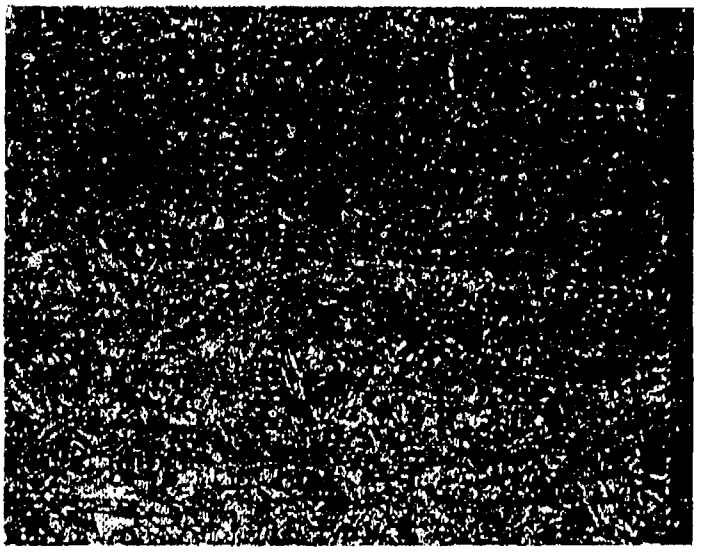

VIEW A
MAGNIFICATION: 200X

VIEW B
MAGNIFICATION: 500X

FIGURE	M & PE LAB NUMBER	M & PE ENGINEER	M & PE TECHNICIAN	DEVICE/PART NUMBER
A-7	27478		D. Dehmer	HY-100 Steel

Microstructure photomicrographs of HY100 steel in cross section at various magnifications, viewing a plane parallel to the sample length. Views A & B illustrate a linear inclusion following etching. Etchant: 3% nital.

RP-532 REV 1/86

Honeywell

DEFENSE SYSTEMS DIVISION
MATERIALS AND PROCESS ENGINEERING

ETR NUMBER 6014

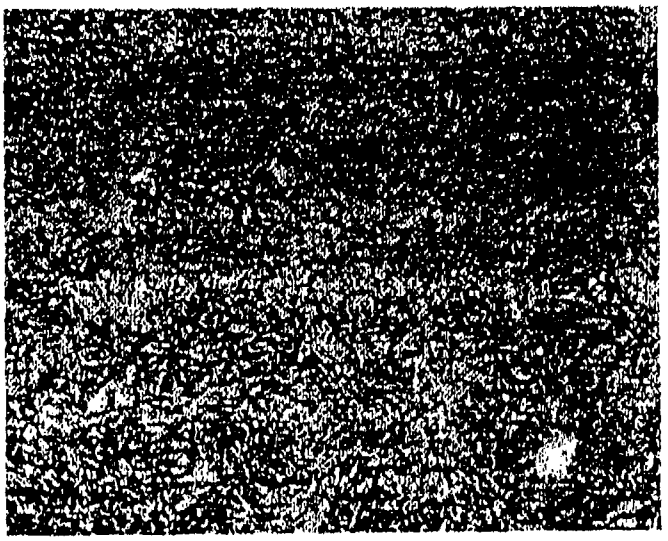

VIEW A
MAGNIFICATION: 200X

VIEW B
MAGNIFICATION: 500X

FIGURE	M & PE LAB NUMBER	M & PE ENGINEER	M & PE TECHNICIAN	DEVICE/PART NUMBER
A-8	27478		D. Dehmer	HY-100 Steel

Microstructure photomicrographs of HY100 steel in cross section at various magnifications, viewing a plane parallel to the plate surface. Views A & B illustrate tempered martensite. Etchant: 3% nital.

HP 532 REV 1-80

Honeywell

DEFENSE SYSTEMS DIVISION
MATERIALS AND PROCESS ENGINEERING

ETR NUMBER 6014

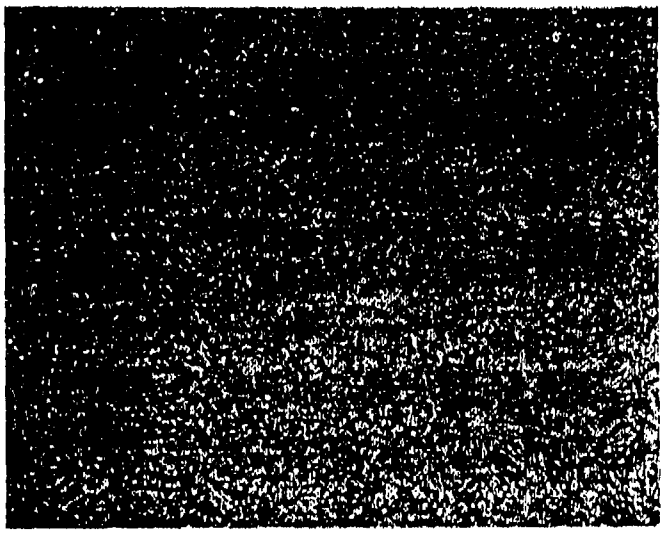

VIEW A
MAGNIFICATION: 200X

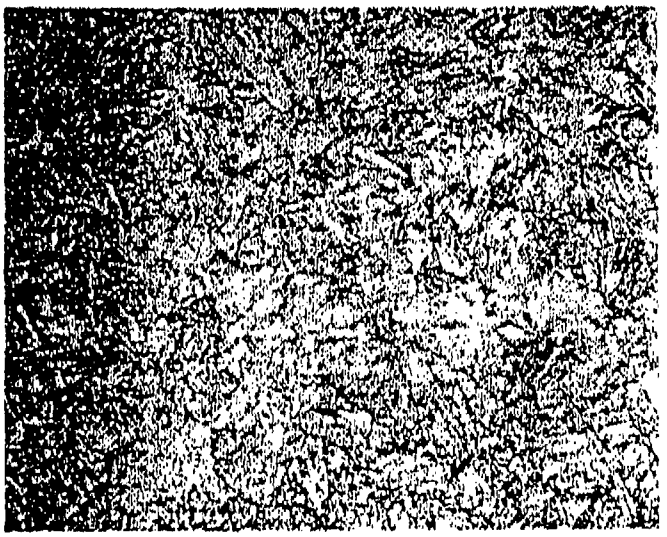

VIEW B
MAGNIFICATION: 500X

FIGURE	M & PE LAB NUMBER	M & PE ENGINEER	M & PE TECHNICIAN	DEVICE PART NUMBER
A-9	27478		D. Dehmer	HY-100 Steel

Microstructure photomicrographs of HY100 steel in cross section at various magnifications, viewing a plane parallel to the sample length. Views A & B illustrate tempered martensite. Etchant: 3% nital.

HP 532 REV 1/86

Honeywell

DEFENSE SYSTEMS DIVISION
MATERIALS AND PROCESS ENGINEERING

FTR NUMBER 6014

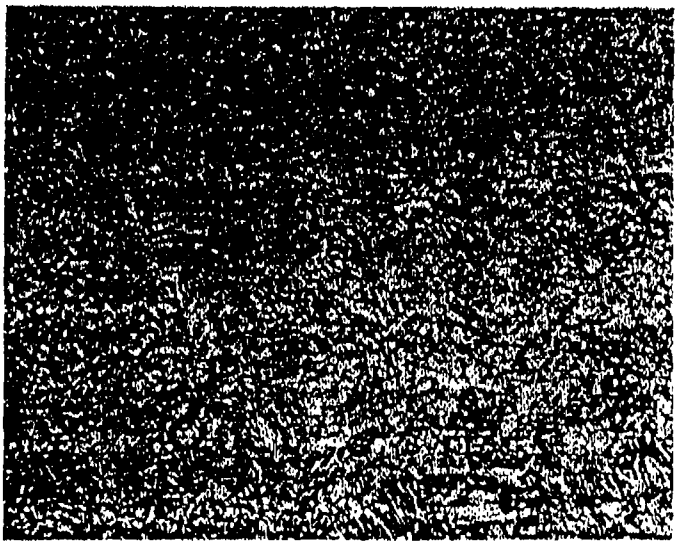

VIEW A
MAGNIFICATION: 200X

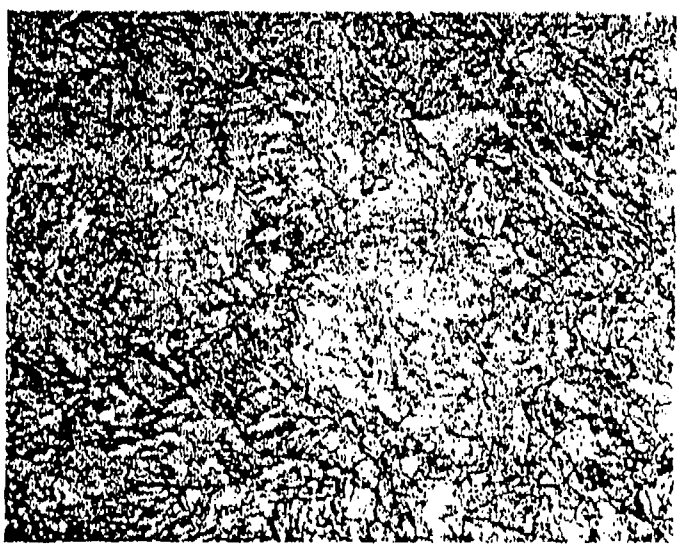

VIEW B
MAGNIFICATION: 500X

FIGURE	M & PE LAB NUMBER	M & PE ENGINEER	M & PE TECHNICIAN	DEVICE PART NUMBER
A-10	27478		D. Dehmer	HY-100 Steel

Microstructure photomicrographs of HY100 steel in cross section at various magnifications, viewing a plane perpendicular to the sample length. Views A & B illustrate tempered martensite. Etchant: 3% nital.

HP 532 REV 1 86

Honeywell DEFENSE SYSTEMS DIVISION
MATERIALS AND PROCESS ENGINEERING

ETR NUMBER 6014

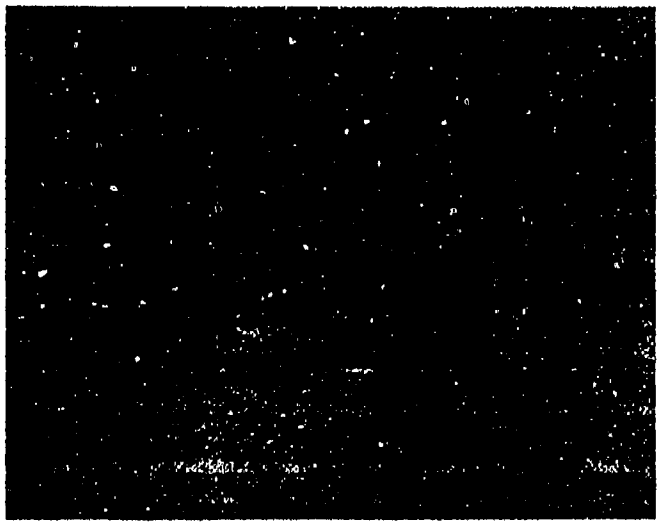

VIEW A
MAGNIFICATION: 200X

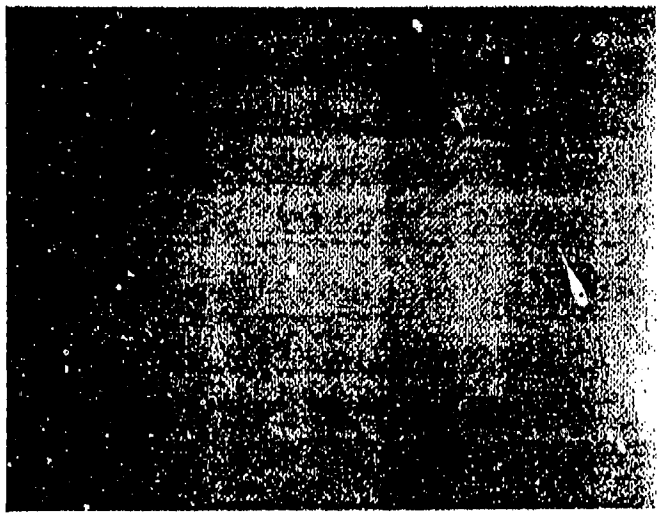

VIEW B
MAGNIFICATION: 200X

FIGURE	M & PE LAB NUMBER	M & PE ENGINEER	M & PE TECHNICIAN	DEVICE/PART NUMBER
A-11	27478		D. Dehmer	HY-130 Steel

Photomicrographs of HY130 steel in cross section, viewing a plane parallel to the sample length. Views A & B illustrate various small sizes of the only inclusion type noted prior to etching. Etchant: 3% nital.

HP-532 REV 1/88

Honeywell

DEFENSE SYSTEMS DIVISION
MATERIALS AND PROCESS ENGINEERING

ETA NUMBER 6014

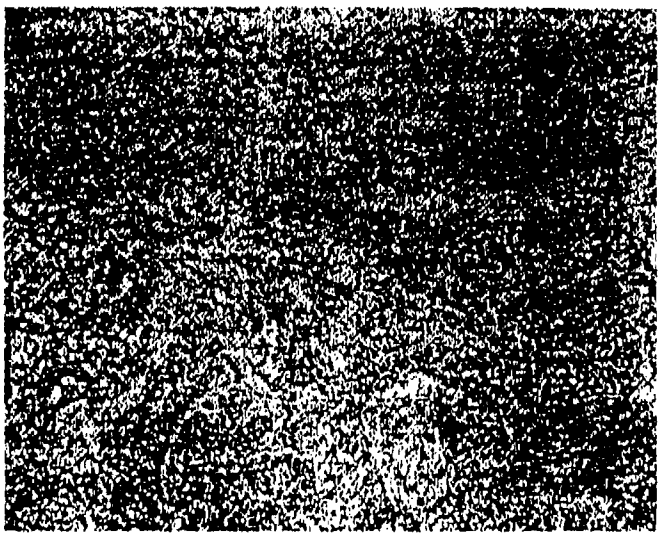

VIEW A
MAGNIFICATION: 200X

VIEW B
MAGNIFICATION: 500X

FIGURE	M & PE LAB NUMBER	M & PE ENGINEER	M & PE TECHNICIAN	DEVICE/PART NUMBER
A-12	27478		D. Dehmer	HY-130 Steel

Microstructure photomicrographs of HY130 steel in cross section at various magnifications, viewing a plane parallel to the plate surface. Views A & B illustrate tempered martensite. Etchant: 3% nital.

HP 532 REV 1-06

Honeywell

DEFENSE SYSTEMS DIVISION
MATERIALS AND PROCESS ENGINEERING

ETR NUMBER 8014

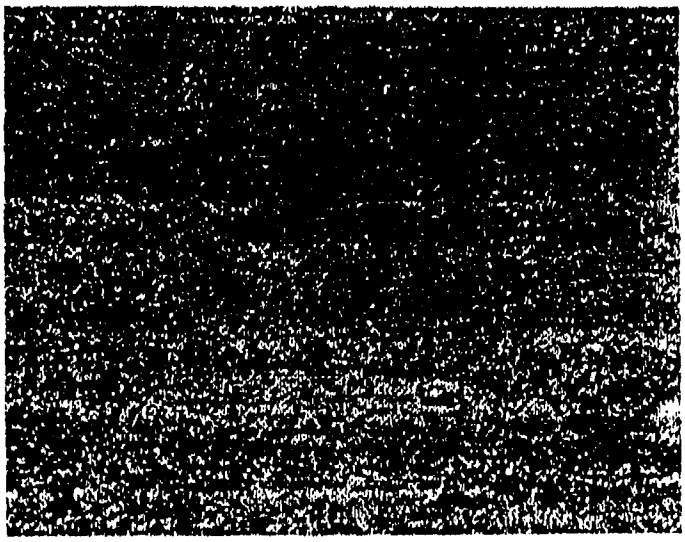

VIEW A
MAGNIFICATION: 200X

VIEW B
MAGNIFICATION: 500X

FIGURE	M & PE LAB NUMBER	M & PE ENGINEER	M & PE TECHNICIAN	DEVICE/PART NUMBER
A-13	27478		D. Dohmer	HY-130 Steel

Microstructure photomicrographs of HY130 steel in cross section at various magnifications, viewing a plane parallel to the sample length. Views A & B illustrato tempered martensite. Etchant: 3% nital.

HP 532 REV 1/86

Honeywell

DEFENSE SYSTEMS DIVISION
MATERIALS AND PROCESS ENGINEERING

ETR NUMBER 6014

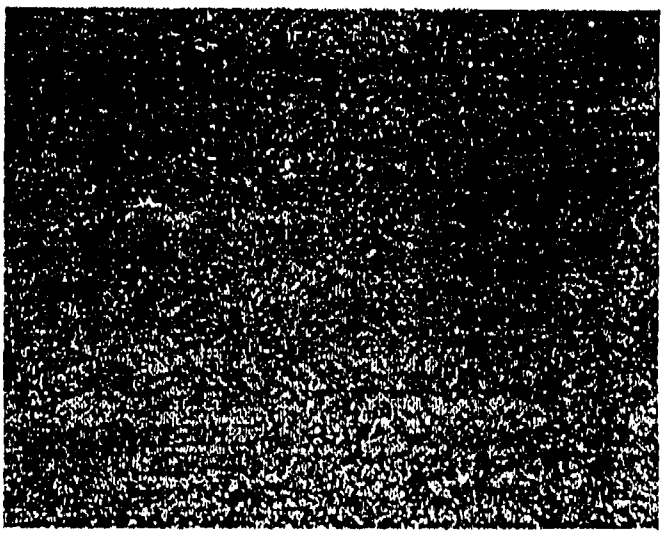

VIEW A
MAGNIFICATION: 200X

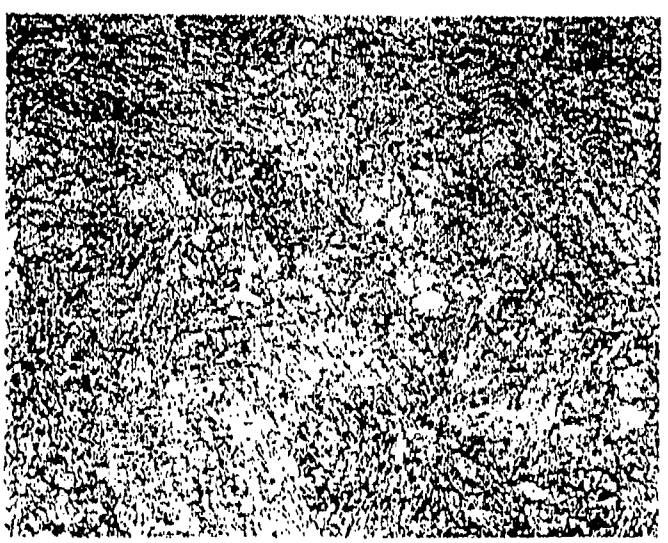

VIEW B
MAGNIFICATION: 500X

FIGURE	M & PE LAB NUMBER	M & PE ENGINEER	M & PE TECHNICIAN	DEVICE/PART NUMBER
A-14	27478		D. Dehmer	HY-130 Steel

Microstructure photomicrographs of HY130 steel in cross section at various magnifications, viewing a plane perpendicular to the sample length. Views A & B illustrate tempered martensite. Etchant: 3% nital.

HP-532 REV 1/86

DISTRIBUTION

	Copies
Chief of Naval Operations Attn: Technical Library Department of the Navy Washington, DC 20350	1
Office of Naval Technology Attn: OCNR-23 OCNR-232 OCNR-213 800 North Quincy Street Ballston Center Towers #1 Room 503 Arlington, VA 22217-5000	1 1 1
Commander Naval Ocean Systems Center Attn: Technical Library San Diego, CA 92152	1
Defense Technical Information Center Cameron Station Alexandria, VA 22314	2
Office of Naval Research Attn: Technical Library 800 North Quincy Street Arlington, VA 22217	1
Sandia National Laboratories Attn: Technical Library Albuquerque, NM 87185	1
Director Defense Nuclear Agency Attn: Technical Library Washington, DC 20305	1
Commanding Officer Naval Coastal Systems Center Attn: Technical Library Panama City, FL 32407	1
Commanding Officer Naval Ordnance Station Attn: Technical Library Indian Head, MD 20640	1
Commanding Officer Naval Ship Weapons Systems Engineering Station Port Hueneme, CA 93043	1
Commanding Officer Naval Undersea Warfare Engineering Station Keyport, WA 98345	1
Commander Naval Weapons Evaluation Facility Kirtland Air Force Base Albuquerque, NM 87117	1
Commander Naval Underwater Systems Center Attn: Technical Library Newport, RI 02840	1
Director Defense Advanced Research Projects Agency Attn: Library Naval Technology Office 1400 Wilson Boulevard Arlington, VA 22209	1 1
Commander Naval Weapons Center Attn: Technical Library Code 3917 China Lake, CA 93555	1 1

DISTRIBUTION (Cont.)

	Copies
Commander Naval Air Systems Command Attn: Technical Library Washington, DC 20361	1
Commander U.S. Army Research and Development Command Attn: Technical Library Dover, NJ 07801	1
Commander Air Force Weapons Laboratory Attn: Technical Library (SUL) Kirtland AFB, NM 87117	1
Commanding Officer Harry Diamond Laboratories Attn: Library 2800 Powder Mill Road Adelphi, MD 20783	1
Director Defense Research and Engineering Attn: Library Washington, DC 20305	1
Lawrence Livermore National Laboratory Attn: Technical Library Livermore, CA 94550	1
Los Alamos National Laboratory Attn: Technical Library P.O. Box 1663 Los Alamos, NM 87544	1

Internal Distribution:	Copies
E231	2
E232	3
R	1
R10	1
R10A	1
R10A (K. Reed)	1
R12	1
R12 (P. Walter)	2
R13	1
R13 (F. Zerilli)	2
U	1